U.S.N.A. --- Trident Scholar project report; no. 375 (2008)

An Essential Protein Repair Enzyme:
INVESTIGATION OF THE MOLECULAR RECOGNITION MECHANISM OF METHIONINE SULFOXIDE REDUCTASE A

by

Midshipman 1/C Joanne D. So, Class of 2008
United States Naval Academy
Annapolis, Maryland

_____
(signature)

Certification of Advisor Approval

Associate Professor Virginia F. Smith
Chemistry Department

_____
(signature)

_____
(date)

Acceptance for the Trident Scholar Committee

Professor Joyce E. Shade
Deputy Director of Research & Scholarship

_____
(signature)

_____
(date)

USNA-1531-2

REPORT DOCUMENTATION PAGE

Form Approved
OMB No. 074-0188

1. AGENCY USE ONLY (Leave blank)	2. REPORT DATE	3. REPORT TYPE AND DATE COVERED
	1 May 2008	

4. TITLE AND SUBTITLE
An Essential Protein Repair Enzyme: Investigation of the Molecular Recognition Mechanism of Methionine Sulfoxide Reductase A

5. FUNDING NUMBERS

6. AUTHOR(S)
So, Joanne D.

7. PERFORMING ORGANIZATION NAME(S) AND ADDRESS(ES)		8. PERFORMING ORGANIZATION REPORT NUMBER

9. SPONSORING/MONITORING AGENCY NAME(S) AND ADDRESS(ES)		10. SPONSORING/MONITORING AGENCY REPORT NUMBER
US Naval Academy Annapolis, MD 21402		Trident Scholar project report no. 375 (2008)

11. SUPPLEMENTARY NOTES

12a. DISTRIBUTION/AVAILABILITY STATEMENT	12b. DISTRIBUTION CODE
This document has been approved for public release; its distribution is UNLIMITED.	

13. ABSTRACT The amino acid methionine is particularly sensitive to damage by reactive oxygen species. The enzyme methionine sulfoxide reductase A (MsrA) is capable of repairing oxidized methionines [Met-(O)] found in a wide range of damaged substrates, ultimately protecting cells against oxidative damage. How MsrA reverses oxygen modifications to these damaged proteins is well known, but very little is known about how MsrA recognizes the damaged proteins in the first place. Unlike most enzymes which carry out reactions on a single target molecule, MsrA can repair damage to a single methionine, a peptide, or an entire protein. This study focused on understanding how MsrA is able to recognize, then ultimately repair such a range of oxidatively modified substrates. We propose that MsrA functions as a molecular chaperone, recognizing overall characteristics of unfolded proteins due to oxidative damage. Enzyme-ligand interactions were studied between MsrA of *E.coli* and four target molecules in their normal and oxidized forms: staphylococcal nuclease, staphylococcal nuclease T62P which has an unfolded structure due to a mutation, a 9-amino acid peptide (KKMVENAKK) derived from staphylococcal nuclease, and the non-steroidal anti-inflammatory drug sulindac. Using the hydrophobic marker 8-anilino-1-naphthalene sulfonic acid (ANS), changes in ANS fluorescence were used to identify changes in the exposed hydrophobic surface area of the protein-ligand complex. The investigation reveals an MsrA target molecule recognition mechanism of weak, but specific hydrophobic interactions enhanced by the presence of a sulfoxide. This study represents the first investigation of the interaction of MsrA with physiologically relevant ligands and has laid the foundation for a novel method of investigating the hydrophobic recognition mechanism of MsrA as a chaperone for oxidatively modified target molecules.

14. SUBJECT TERMS	15. NUMBER OF PAGES
Methionine sulfoxide reductase, chaperone, enzyme, fluorescence spectroscopy, methionine oxidation	65
	16. PRICE CODE

17. SECURITY CLASSIFICATION OF REPORT	18. SECURITY CLASSIFICATION OF THIS PAGE	19. SECURITY CLASSIFICATION OF ABSTRACT	20. LIMITATION OF ABSTRACT

Abstract

The amino acid methionine is particularly sensitive to damage by reactive oxygen species. The enzyme methionine sulfoxide reductase A (MsrA) is capable of repairing oxidized methionines [Met-(O)] found in a wide range of damaged substrates, ultimately protecting cells against oxidative damage. How MsrA reverses oxygen modifications to these damaged proteins is well known, but very little is known about how MsrA recognizes the damaged proteins in the first place. Unlike most enzymes which carry out reactions on a single target molecule, MsrA can repair damage to a single methionine, a peptide, or an entire protein. This study focused on understanding how MsrA is able to recognize, then ultimately repair such a range of oxidatively modified substrates. We propose that MsrA functions as a molecular chaperone, recognizing overall characteristics of unfolded proteins due to oxidative damage. Enzyme-ligand interactions were studied between MsrA of *E.coli* and four target molecules in their normal and oxidized forms: staphylococcal nuclease, staphylococcal nuclease T62P which has an unfolded structure due to a mutation, a 9-amino acid peptide (KKMVENAKK) derived from staphylococcal nuclease, and the non-steroidal anti-inflammatory drug sulindac. Using the hydrophobic marker 8-anilino-1-naphthalene sulfonic acid (ANS), changes in ANS fluorescence were used to identify changes in the exposed hydrophobic surface area of the protein-ligand complex. The investigation reveals an MsrA target molecule recognition mechanism of weak, but specific hydrophobic interactions enhanced by the presence of a sulfoxide. This study represents the first investigation of the interaction of MsrA with physiologically relevant ligands and has laid the foundation for a novel method of investigating the hydrophobic recognition mechanism of MsrA as a chaperone for oxidatively modified target molecules.

Keywords: Methionine sulfoxide reductase, chaperone, enzyme, fluorescence spectroscopy, methionine oxidation

Acknowledgements

I would like to extend my sincere and utmost gratitude to Dr. Virginia Smith for her guidance and mentorship throughout this research endeavor and beyond it.

I would like to thank my parents, John and Tonette So, my grandparents Fernando and Pacita Diaz, and Lutgarda So—by their example, I learned the value of perseverance and hard-work.

Special thanks to:

Mrs. Lynne Fenwick for gracious and dedicated administrative and logistical support.

Dr. Bill Stephen, Dr. Jamie Schlessman, Ms. Kristen Selde, and Ms. Jackie Brown of the U.S. Naval Academy Chemistry Department for technical support.

Dr. Danny Morse for reminding me of the thousands of times Thomas Edison failed before he found success.

Professors Daniel O'Sullivan, Kiriakos Kiriakidis, and Ernie Tucker of the Trident Scholar Committee for their interest and support of this project.

Mrs. Karen Flecknoe, Mrs. Cindi Gallagher, and Mr. Brendan Beers of the Multimedia Support Center Graphics Department.

Funding was provided by the Office of Naval Research, the Trident Scholar Program, the USNA Chemistry Department, and the Cottrell College Research Award to V.F.S.

TABLE OF CONTENTS

LIST OF FIGURES AND TABLES

Background

An unforgiving reality of life in an aerobic environment is cell damage caused by reactive oxygen species (ROS)—by-products of normal cellular metabolism and oxidative stress. Numerous studies have revealed pathophysiological evidence that strongly links oxidative damage to neurodegenerative and age-related diseases such as Alzheimer's disease, Parkinson's disease, Amyotrophic Lateral Sclerosis (Lou Gehrig's Disease), emphysema, and arthritis (*1*). These reactive species such as hydrogen peroxide, superoxide anions, and hydroxyl radicals oxidize proteins and convert lipid and carbohydrate derivatives to compounds that react with functional groups on proteins (*2*). Methionine and cysteine amino acid residues are particularly sensitive to oxidation resulting in loss of function; however, the damage of oxidation can be reversed, ultimately resulting in complete functional recovery. Methionine and cysteine are the only amino acids that can be reversibly oxidized under physiological conditions.

It was only about 25 years ago that the enzyme responsible for repairing and protecting cells from oxidative damage was discovered. The gene encoding this enzyme, methionine sulfoxide reductase A (MsrA), has been found in all living organisms sequenced to date. MsrA was discovered in studies on the biological activity of ribosomal protein L12 of *Escherichia coli.* All activity of L12 was lost when three or more methionine residues were oxidized. In these studies, it was shown that these *E. coli* extracts contained an enzymatic activity, MsrA, which could repair this oxidative damage and reduce the oxidized methionines (*3*). The *E.coli* MsrA gene was cloned to perform structural and genetic studies and to determine the significance of the physiological role of the enzyme. It was reported that overexpression of MsrA in human T-lymphocyte

cells protected them against oxidative stress. A further study on mice reported that MsrA knockout in mice had a shorter life span, were more sensitive to hyperbaric oxygen and had a neurological defect that resulted in abnormal walking. Mutations leading to a loss of MsrA activity in mice lead to a 40% decrease in maximum life span, while overexpression of MsrA in flies leads to a nearly doubling of the lifespan (*4*).

Beyond protection against oxidative stress in eukaryotes, MsrA plays a significant function in the infection of cells by pathogenic bacteria. These bacteria which include *Streptococcus pneumoniae*, *Neisseria gonorrhoeae, Escherichia coli,* and *Haemophilus influenzae* depend on adhesins to bind to host tissues. In these bacteria, MsrA maintains the functionality of these adhesins that is so essential to bacterial pathogenicity. A strain of *Streptococcus pneumoniae* containing a mutated form of MsrA had a decreased ability to bind to lung epithelial cells and human vein epithelial cells (*5*).

The focus of this research is to determine the recognition mechanism of MsrA for proteins denatured by the oxidation of methionine. This research is essential for developing a complete understanding of the kinetics and mechanisms by which MsrA recognizes oxidized proteins which may then give significant insight into the development of novel drugs that would serve as catalytic anti-oxidants using the Msr system. These drugs would serve as a vanguard for the effective treatment of the neurodegenerative human diseases associated with aging and oxidative damage. Furthermore, as eubacteria become increasingly resistant to conventional antibiotics, the investigation and understanding of MsrA function in adhesins could serve as a new antibacterial enzyme target as a defense against pathogenicity.

While it is not always understood how methionine oxidation changes the

biological activity of a protein, oxidation is known in some cases to destabilize a protein's native structure (*6*). It is well known that side chain substitution can have profound effects on protein stability and structure. In effect, oxidation can be regarded as a chemical 'mutagenesis' which substitutes the methionine side chain with methionine sulfoxide, a larger and more polar side chain. It should not be surprising that it can greatly disrupt protein structure and stability (*7*).

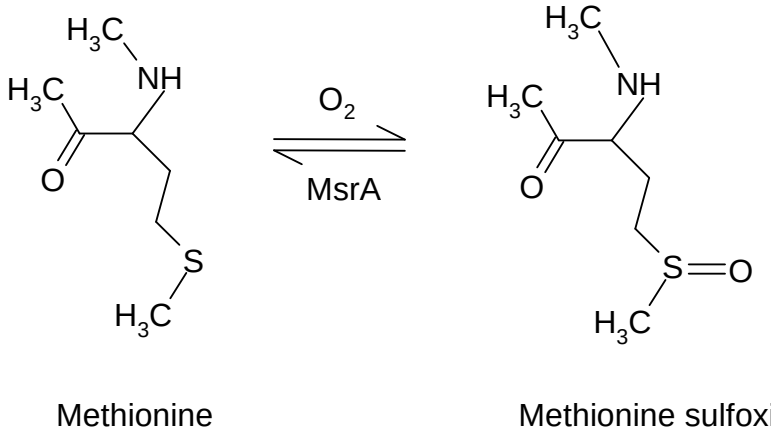

Figure 1. The amino acid methionine is modified by oxygen and becomes methionine sulfoxide [Met(O)].

MsrA, which specifically reduces S-enantiomeric sulfoxides of denatured proteins, has an unusually broad substrate specificity and it is still not completely understood how MsrA is able to interact with and repair such a range of proteins. The proposed roles of MsrA as essential to the repair of oxidative damage, as a scavenger of reactive oxidative species, and as a regulator of the biological activity of a protein, have been thoroughly established. How MsrA is able to recognize proteins that contain oxidized methionines [Met(O)] in the first place is still unknown.

Structure and Catalytic Mechanism of MsrA

Basic Structure and Sequence

MsrA (Figure 2) of *E. coli* is a small monomeric protein of about 23 kDa. Analysis of MsrA reveals a unique fold with a large proportion of coils and highlights the roles of several residues that might be involved in the catalytic process. The MsrA model possesses a single domain described as an α/β roll (*1*). The N and C terminal regions are highly flexible. Interestingly, MsrA has been cloned from many sources including bacteria, yeast, bovine, plant, and human cells, and the protein is very highly conserved from these sources (*8*). There is a 67% sequence identity between the *E.coli* and human MsrA (*2*).

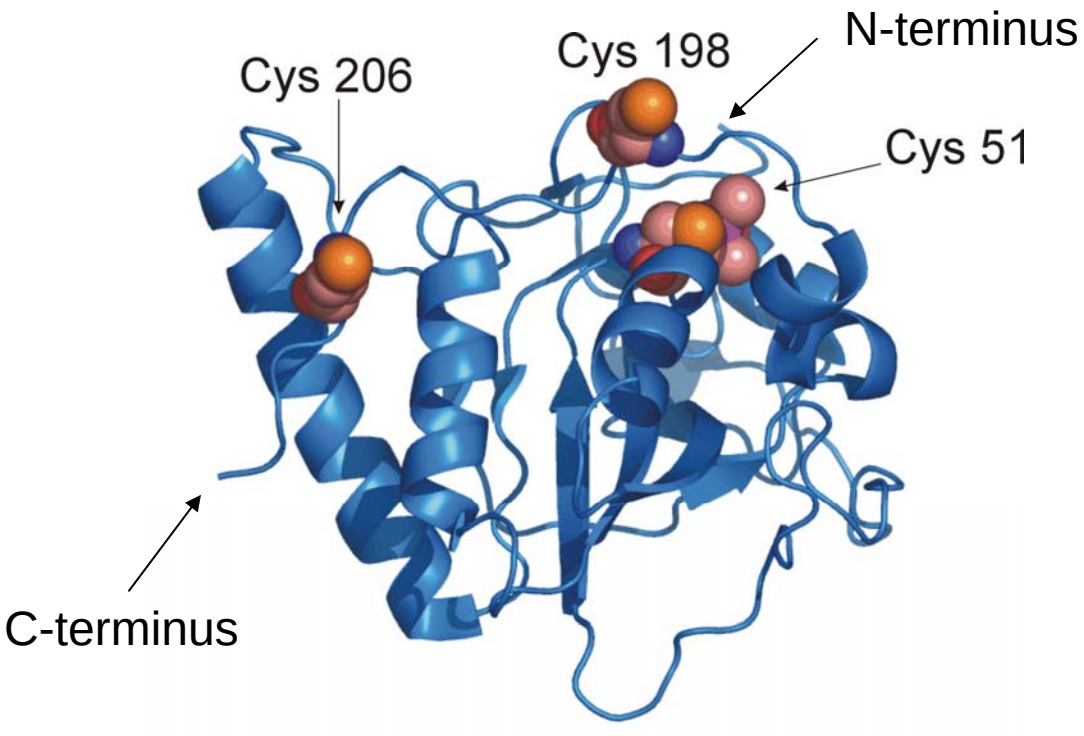

Figure 2. Three-dimensional structure of methionine sulfoxide reductase A (MsrA) with catalytic cysteine residues highlighted. The image was generated from PDB file 1FF3 (*1*) using PyMOL Molecular Graphics System, Version 0.97 (*9*).

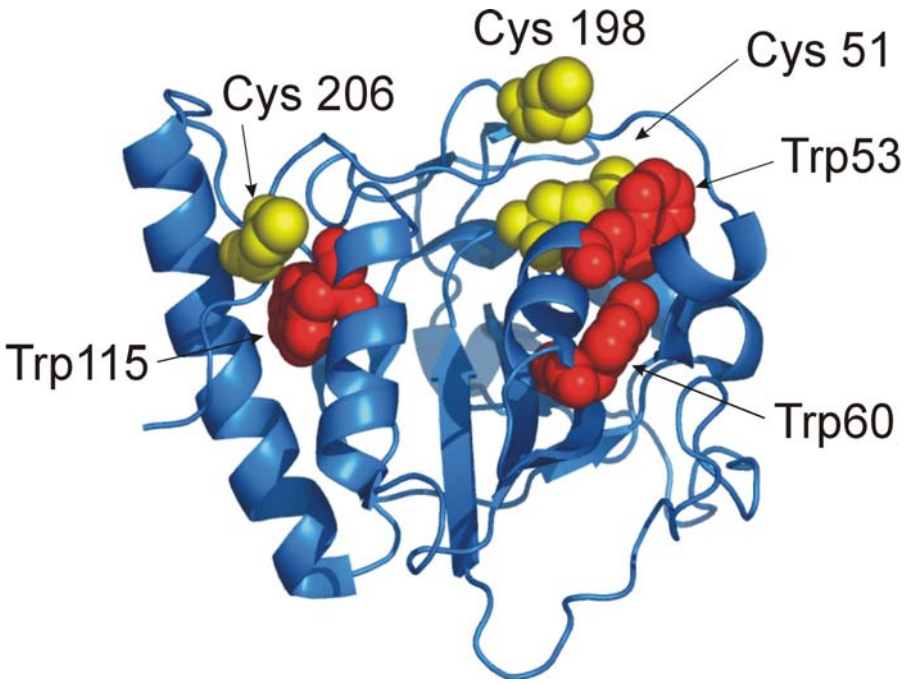

Figure 3. Three-dimensional structure of methionine sulfoxide reductase A with active-site cysteine residues and tryptophans designated (*1*,*9*).

Catalytic Mechanism of Repair

The cysteine residues of MsrA are essential for catalytic activity (*10*). The cysteine contained at the highly conserved N-terminal amino acid motif, GCFWG, is found in all MsrA sequences. Figure 4 diagrams the catalytic mechanism of MsrA of *E.coli* in reducing oxidized methionines.

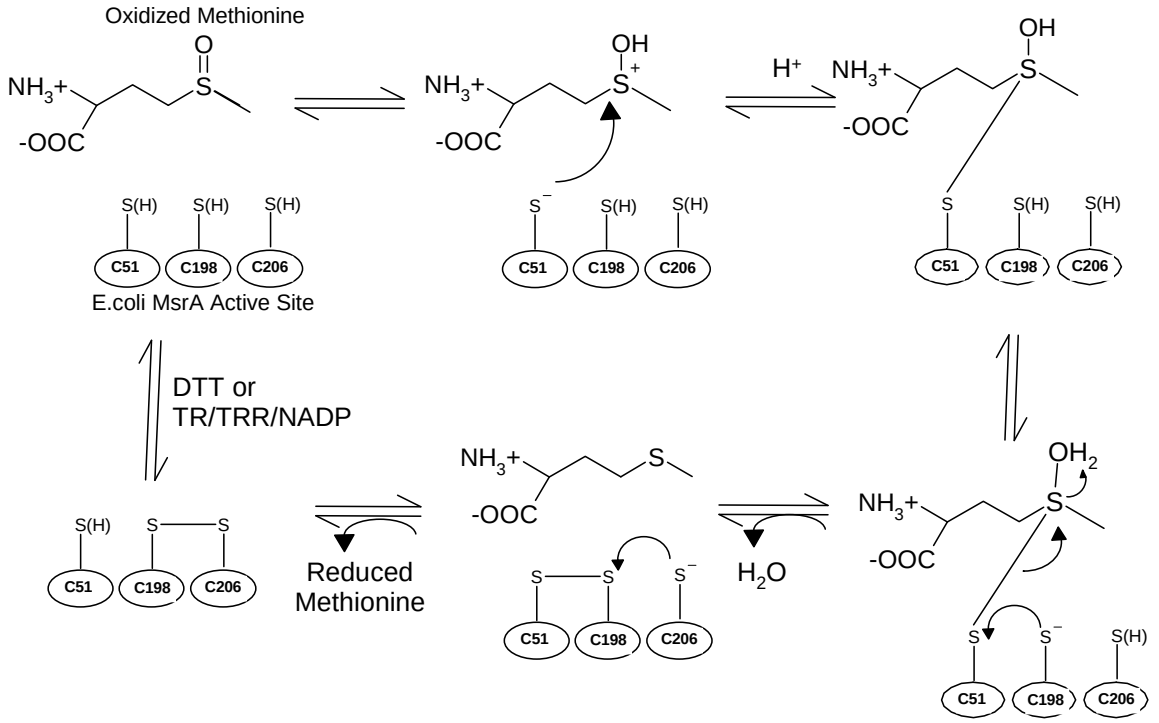

Figure 4. Proposed reaction mechanism for MsrA catalysis. Protonation of Met(O) leads to the formation of a sulfonium ion. With sulfoxide protonation, cysteine 51 attacks the sulfur atom of the sulfonium ion, leading to the formation of a covalent intermediate. Breakdown of the complex is facilitated by proton transfer and the attack on cysteine 51 by cysteine 198. Return to a fully reduced state is facilitated by thiol-disulfide exchange using either dithiothreitol or reduced thioredoxin (*3*).

Hydropathy of MsrA

The hydropathy index of an amino acid is a number that represents the hydrophobic or hydrophilic nature of the amino acid. The scale ranges from -4.6 to +4.6 with more negative values representing hydrophilic character and positive values representing hydrophobic character.

Table 1. Kyte-Doolittle Hydropathy Index

Increasing Hydrophobicity ↑	Isoleucine	4.5
	Valine	4.2
	Leucine	3.8
	Phenylalanine	2.8
	Cysteine	2.5
	Methionine	1.9
	Alanine	1.8
	Glycine	-0.4
	Threonine	-0.7
	Serine	-0.8
	Tryptophan	-0.9
	Tyrosine	-1.3
	Proline	-1.6
	Histidine	-3.2
	Asparagine	-3.5
	Aspartic acid	-3.5
	Glutamine	-3.5
	Glutamic acid	-3.5
	Lysine	-3.9
	Arginine	-4.5

The Kyte-Doolittle hydropathy plot predicts hydrophobic regions of a protein based on the protein's primary sequence. A Kyte-Doolittle hydropathy plot of MsrA was generated using the primary sequence derived from Protein Data Base (PDB) crystal structure code 1ff3 of MsrA of E.*coli*.

Kyte-Doolittle Hydropathy Plot of MsrA of *E.coli*

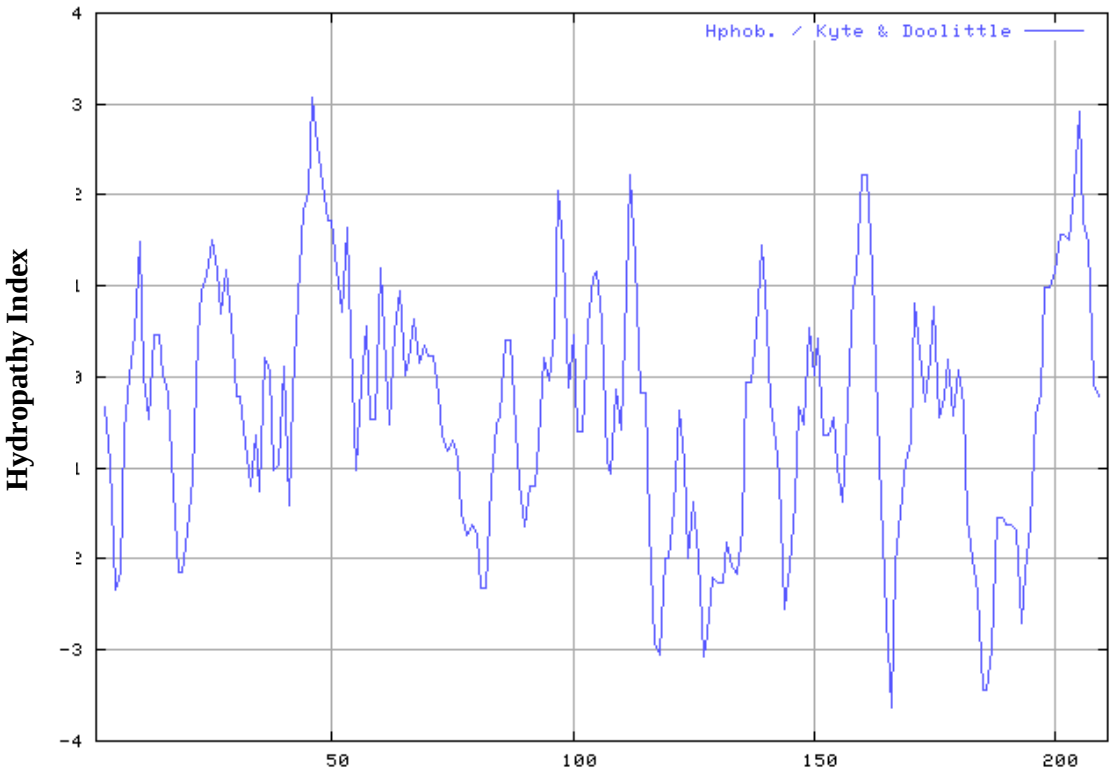

Figure 5. Kyte-Doolittle Hydropathy plot of MsrA of E.*coli* generated from PDB file 1ff3 (*11*). Window size=5, Max=3.080, min=-3.640. Sequence length=211.
MsrA Sequence, N-terminus→C-terminus: SLFDKKHLVSPADALPGRNTPMPVATLHAVNGHS MTNVPDGMEIAIFAMGCFWGVERLFWQLPGVYSTAAGYTGGYTPNPTYREVCSGDTGHAE AVRIVYDPSVISYEQLLQVFWENHDPAQGMRQGNDHGTQYRSAIYPLTPEQDAAARASLERF QAAMLAADDDRHITTEIANATPFYYAEDDHQQYLHKNPYGYCGIGGIGVCLPPEA

MsrA is comprised of only 35.1% ordered α-helical and β-strand structure while the remaining residues of the protein consist of irregular loop structures (*1)*. The absence of structure in the long N- and C-ends is a significant feature of MsrA. The long, flexible coils of the N-terminus (residues Ser-1-Met-42) and C-terminus (residues Glu-182-Ala-211) regions of MsrA are particularly hydrophobic based on the Kyte-Doolittle hydropathy plot. The sequence of residues 48-54 of the protein Msr (PMSR) family is highly conserved, containing the first catalytic cysteine residue essential to the reduction

of methionine sulfoxide. Of note, this sequence is the most hydrophobic of all regions of MsrA.

Analysis of the three-dimensional structure of MsrA confirms that the active site Cys-51 is located in a solvent-exposed region of the protein. It is shaped like a largely opened basin whose surface is mainly covered with aromatic amino acids. These side chains are either conserved or replaced by equivalent aromatic side chains. The presence of these side chains does not prevent access to the catalytic cysteine (*1*).

Investigation of Hydrophobic Substrate Recognition Mechanism

Based on the sequence and structural properties of MsrA, particularly at the highly conserved active site region of the protein, we investigated the hydrophobic interactions of MsrA with four specifically chosen target molecules in their reduced and oxidized forms: a 9-amino acid peptide (KKMVENAKK) derived from staphylococcal nuclease, the non-steroidal, anti-inflammatory drug Sulindac, wild-type staphylococcal nuclease, and staphylococcal nuclease T62P which has an unfolded structure due to a mutation. Proteins modified by oxidative damage become denatured—or unfolded—exposing hydrophobic and backbone regions of the protein that would otherwise be buried within the protein's normal structure. Using the fluorescent marker 8-anilino-1-naphthalene sulfonic acid, the affinity of MsrA for each of the chosen substrates was investigated, giving insight into the nature of the hydrophobic recognition mechanism of MsrA. ANS is a valuable probe for the detection and analysis of protein conformational changes as the fluorescent marker binds non-covalently to hydrophobic aminoacyl surfaces.

Experimental Ligands

8-anilino-1-naphthalene sulfonic acid (ANS)

8-anilino-1-naphthalene sulfonic acid (MW=299.34) binds to hydrophobic clusters of aminoacyl residues (*13*). ANS is a charged fluorescent dye and functions as an extrinsic fluorescence reporter of the exposed hydrophobic surface area of a protein. ANS fluoresces only when bound to a hydrophobic surface on a protein. The dye is excited at 370 nm and the equilibrium emission is measured at 420 nm.

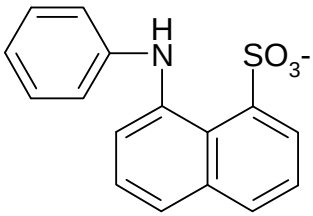

8-anilino-1-naphthalene sulfonic acid (ANS)

Figure 6. Structure of 8-anilino-1-naphthalene sulfonic acid.

9-amino Acid Peptide (KKMVENAKK)

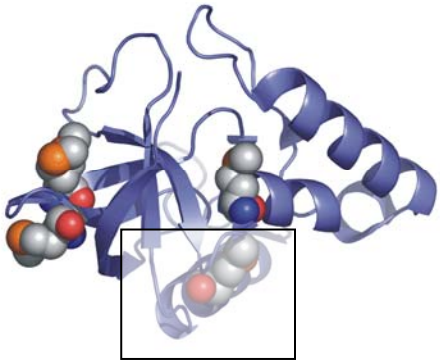

Figure 7. Wild type staphylococcal nuclease with highlighted alpha helix from which the 9-amino acid peptide KKMVENAKK was derived and synthesized.

The sequence for the 9-amino acid peptide KKMVENAKK (MW=1117.0) was derived from wild type staph nuclease from the first alpha helix of the sequence. Oxidation of the methionine from this sequence renders significant loss in structure of the native protein. The sequence was chosen also because it contained no tryptophan so changes only in MsrA during protein-peptide interaction could be monitored by intrinsic tryptophan fluorescence.

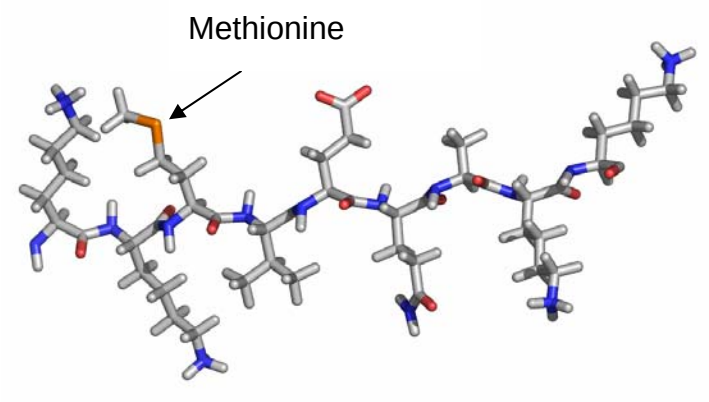

Figure 8. The 9-amino acid KKMVENAKK was derived and synthesized. This image is intended to convey sequence information and is not based on the experimentally determined structure. Image generated using PyMOL Molecular Graphics System, Version 0.97 (*9*).

The propensity of the peptide to form a helix and assume some form of structure was determined using AGADIR™ (*14*). AGADIR™ predicts peptide helicity based on data obtained from specifically selected peptide structures studied by nuclear magnetic resonance and circular dichroism spectroscopy.

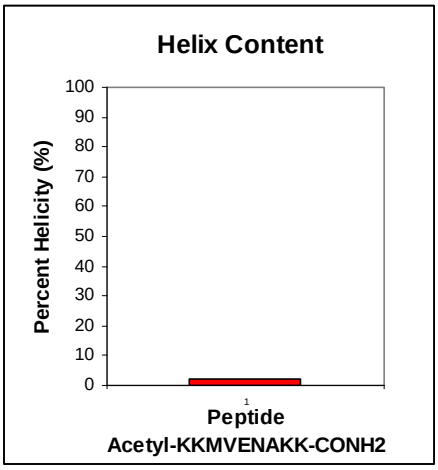

The following parameters were entered into the program based on experimental conditions:

Buffering solution:	Phosphate Buffered Saline
pH:	7.3
Ionic Strength:	0.25
Temperature:	15°C
N-terminus:	Acetylated
C-terminus:	Amidated

Predicted Helicity: 1.97%

Figure 9. AGADIR™ predicted helicity of the peptide KKMVENAKK.

The AGADIR™ plot of the low helical propensity for the SN-derived peptide (1.97%) verifies that the peptide is natively unstructured.

Sulindac

Sulindac (MW=356.41) is a non-steroidal anti-inflammatory drug. It contains a sulfoxide and functions as a pro-drug. Biologically, the liver reduces sulindac to sulindac sulfide which then functions as an active inhibitor of cyclooxygenases 1 and 2 thus exerting anti-inflammatory activity.

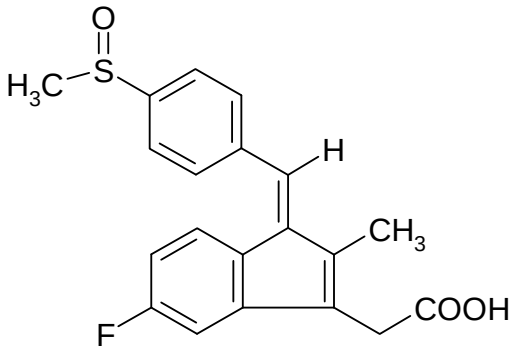

Sulindac

Figure 10. Structure of sulindac, an NSAID COX-1 and COX-2 inhibitor and known substrate for MsrA.

Sulindac and other non-steroidal anti-inflammatory drugs have received considerable attention because of their activity against colorectal cancer (*3*). Sulindac, a known substrate for MsrA, could function as a potential catalytic anti-oxidant and has been investigated in its role for the treatment of Alzheimer's disease. It was studied in these experiments to investigate the capability and affinity of MsrA to recognize sulfoxides in non-protein molecules.

Sulindac sulfide

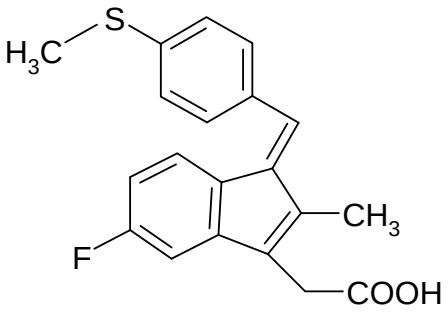

Sulindac sulfide

Figure 11. Structure of sulindac sulfide, the active form of the pro-drug sulindac.

The interactions of MsrA with sulindac sulfide (MW=348.41), the biologically active form of sulindac *in vivo*, were investigated to assess the recognition affinity of MsrA for the apolar structure of the molecule when a sulfoxide modification is not present.

Wild Type Staphylococcal Nuclease and Staph Nuclease T62P (SN T62P)

Staphylococcal nuclease (MW=16811) is an enzyme of *Staphylococcus aureus* which functions to cleave phosphodiester bonds of nucleic acids. This protein was chosen as a target molecule for these experiments to demonstrate the ability of MsrA to repair damaged full protein substrates. Wild type staph nuclease contains four methionines.

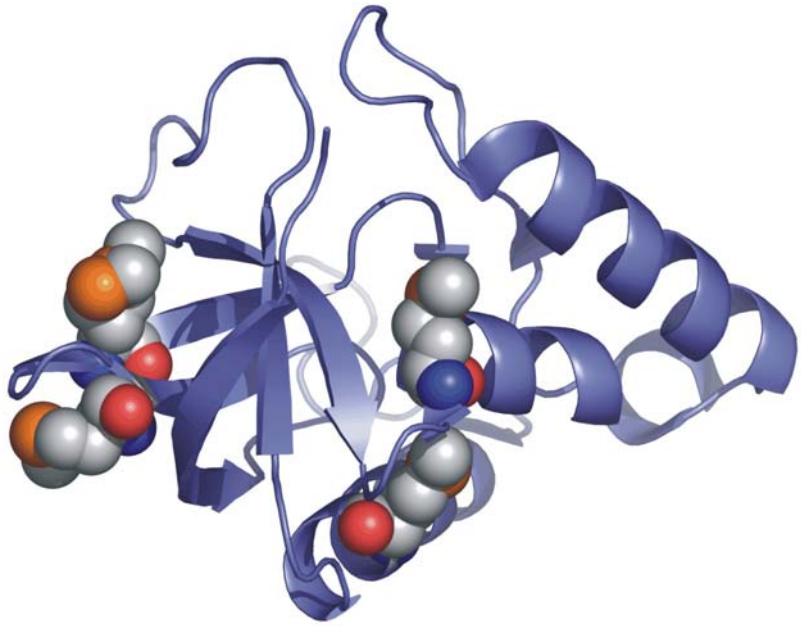

Figure 12. Wild type staphylococcal nuclease. Image was generated from PDB file 1EYD (*12*) using PyMOL Molecular Graphics System, Version 0.97 (*9*). Methionines are designated by ball clusters.

Staphylococcal nuclease T62P is derived from the thermodynamically stable wild type staph nuclease and has been made to be intrinsically unstructured by replacing threonine with proline in the α-helix of staph nuclease (*12*). SN T62P assumes a natively unfolded structure due to this site-directed mutagenesis.

Experimental Investigation
(See Appendices for detailed protocols)

Growth and Purification of MsrA

Genetically modified BL21-DE3 cells of *E.coli* were selected for the overproduction of the recombinant glutathionine-S-transferase (GST)-MsrA fusion protein. An upscale culture was performed in luria broth and ampicillin. The *lac*-inducer isopropyl β-D-1-thiogalactopyranoside (IPTG) was added to the final upscale culture to promote protein overproduction. The *E.coli* cells were harvested, pelleted and stored at -80°C. The cells were lysed with phosphate bacterial protein extraction reagent, releasing intracellular contents. The fusion protein was isolated by a glutathione affinity column and eluted from the column with tris-glutathione. The fusion protein was cleaved with thrombin protease. After overnight incubation with benzamidine and glutathione resin, pure MsrA was isolated. Protein concentration was determined using the experimentally determined extinction coefficient ε=34,600 $M^{-1}cm^{-1}$. Protein identity and molecular weight were determined by sodium dodecyl sulfate polyacrylamide gel electrophoresis (SDS-PAGE).

Preparation of Ligands

All target molecules were prepared in PBS, pH=7.3 to ensure the titration samples were buffer matched for fluorescence equilibrium experiments. The sources of the target molecules were: ANS, Sigma™; SN peptides (oxidized and reduced), SynPep™; Sulindac, Sigma™; Sulindac sulfide, Sigma™; WT SN and SN T62P (oxidized and reduced) were prepared at USNA.

Extrinsic Fluorescence Experiment Conditions and Parameters

Equilibrium fluorescence measurement experiments were performed on the

Horiba Jobin-Yvon Fluorolog-3™ fluorimeter. The fluorimeter is equipped with a temperature controlled cell holder to maintain experimental samples at a constant 15°C. Temperature changes affect the viscosity of the solution sample which affects the number of molecular collisions of the fluorophore with molecules of the solvent. This affects the overall observed fluorescence signal. All experimental samples were buffered in phosphate buffered saline, pH=7.3. Sample fluorescence was measured in a quartz cuvette cell from Hellma™.

Table 2. Fluorimeter Experimental Parameters

PARAMETER	SETTING
Experiment Type	Time-base Acquisition
Time(s)	30.00
Excitation Wavelength (nm)	370
Emission Wavelength (nm)	420
Increment (s)	1.0
Integration Time (s)	1.0
Signals	S
Slit	4 nm Bandpass
HV(on)	950

ANS and Ligand Competition Reactions for MsrA Binding Site

The goal of this research endeavor was to investigate an MsrA hydrophobic recognition mechanism in support of the protein's role as a chaperone. ANS is a valuable probe for the detection and analysis of protein conformational changes as the fluorescent marker binds non-covalently to hydrophobic aminoacyl surfaces. In this experimental design, the function of ANS is two-fold: (1) to report on the structural changes in MsrA upon ligand interaction and (2) to serve as a hydrophobic ligand reference standard for a series of ligand binding experiments to determine MsrA affinity for various target molecules.

ANS Binding Experiments

The fluorescent reporter ANS was used to study conformational changes—exposure of hydrophobic regions—of MsrA as the enzyme interacted with each target molecule. The target molecule species were manually titrated into the temperature stabilized sample containing MsrA and ANS in PBS in the thermostatted cell holder of the fluorimeter. The sample was excited at 370 nm and the fluorescence emission of ANS was measured at 420 nm. The fluorescent emission intensity is proportional to the amount of ANS bound to hydrophobic regions of protein. This information was used to determine a dissociation constant (K_d in μM units) for the MsrA-ligand complex. The dissociation constant is an equilibrium constant that gives insight on the affinity of two molecules to form a complex, in this case, MsrA and the specific target molecule. The smaller the K_d value, the more affinity two molecules will have to form a complex—the molecules only begin to dissociate at a lower ligand concentration.

Control experiments were performed by measuring the equilibrium fluorescence intensity of ANS and the titrated target molecules in the absence of MsrA. These controls also corrected for dilution effects of titration. Experimental titrations refer to the target compound titrations into the sample cell already containing thermally equilibrated MsrA and ANS. The control experiment fluorescence values were subtracted from the experimental titrations to determine the corrected hydrophobic surface exposure changes in MsrA alone. The corrected data also gives insight on the identity of the bound ligand, defined by the change in fluorescence of ANS. Experiments were performed at [MsrA] = 1 μM and repeated at low (15 μM) and high (100 μM/300 μM) concentrations of ANS.

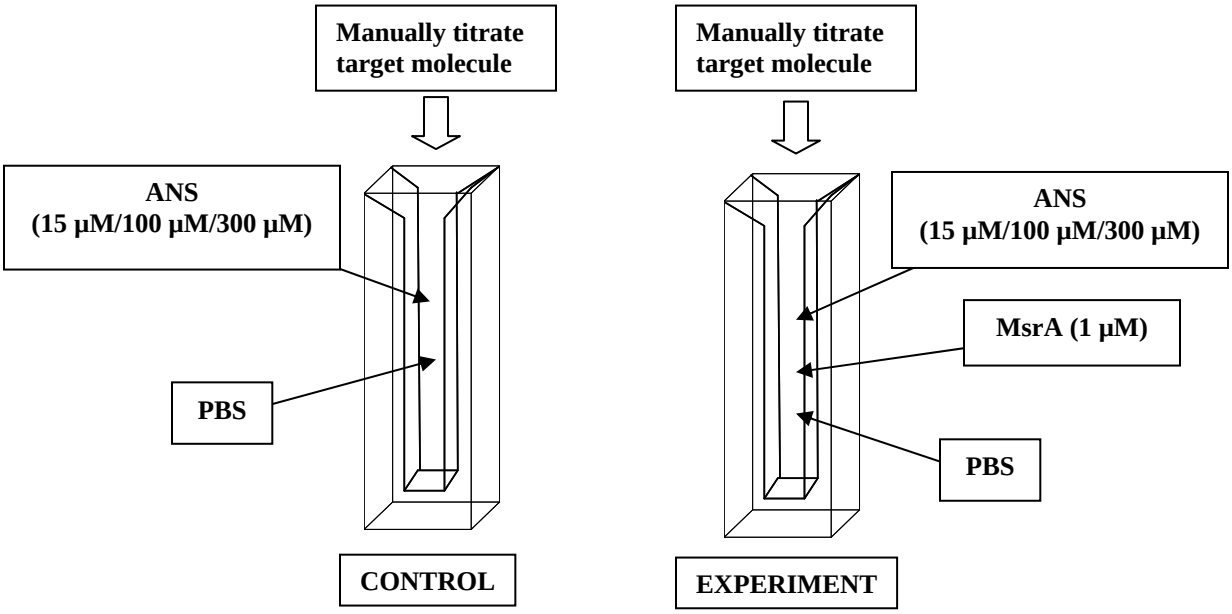

Figure 13. Schematic of control and experimental samples.

Data Analysis and Results

Calculation of the Dissociation Constant (K_d)

In protein biochemistry, the dissociation constant is used to determine the propensity of a protein to bind a ligand. Protein-ligand complex formation is described as an equilibrium, two-state process:

$$\mathbf{[P \bullet L] \rightleftharpoons [P] + [L]}$$

where **[P]** = unbound protein, **[L]** = unbound ligand, and **[P • L]** = complex of protein and ligand. The dissociation constant is described by the following identity:

$$\mathbf{K_d = \frac{[P][L]}{[P \bullet L]}}$$

At equilibrium: the greater the concentration of the protein-ligand complex (denominator) the greater the affinity for complex formation. A complex that is tightly bound will have a small dissociation constant.

Determination of MsrA-ANS Dissociation Constant

Extrinsic fluorescence equilibrium measurements of the interaction of MsrA with ANS produced a titration binding curve with fluorescent intensity as a function of ANS concentration. Figure 14.1 is a fluorescence plot of the uncorrected ANS-MsrA experimental data and superimposed control.

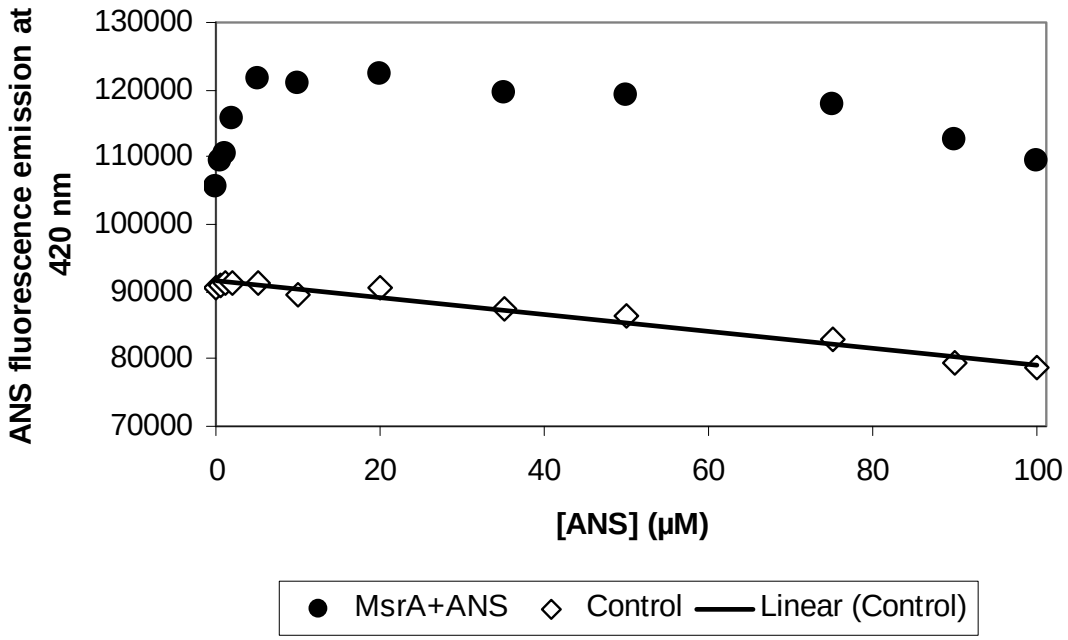

Figure 14.1. Determination of MsrA-ANS dissociation constant (K_d).

The corrected fluorescence emission of ANS was determined by subtracting control values from experimental values of the MsrA-ANS interaction. Figure 14.2 is a plot of the corrected data.

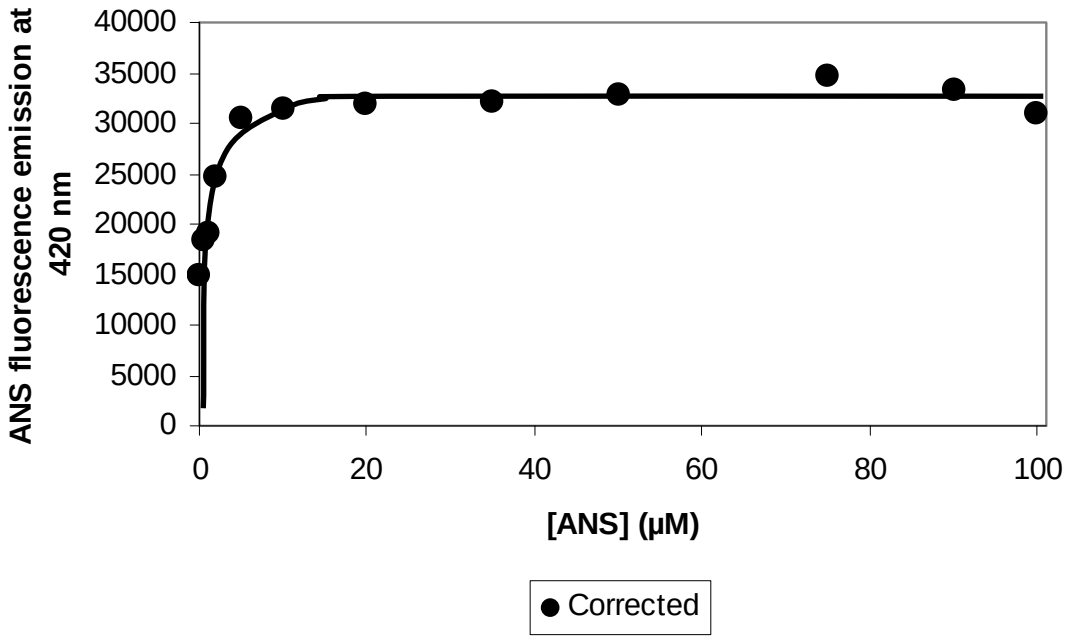

Figure 14.2. Plot of corrected MsrA-ANS fluorescence data for determination of dissociation constant, K_d. The dissociation constant of the MsrA-ANS complex was determined by a hyperbolic fit of the data points. $K_d = 1.78 \pm 0.46$ μM.

Using the program SigmaPlot™, the corrected data points were fit with a rectangular hyperbola of the form $y= B_{MAX}*[ANS]/(K_d + [ANS])$, where B_{MAX} is the saturation (maximum) fluorescence of the titration set. A K_d of 1.78±0.46 μM was obtained from the hyperbolic fit.

Scatchard Linear Transformation

From the experiments for determining the association affinity of the MsrA-ANS complex, we were able to derive the number of hydrophobic binding sites on MsrA. The equilibrium fluorescence emission data from the determination of K_d for the MsrA-ANS complex was linearly transformed to fit a Scatchard plot model. The Scatchard analysis is a method of linearizing data from a saturation binding experiment (*15*) where the regression fit of the data gives:

x-intercept = number of ligand binding sites on protein
slope = $-1/ K_d$

Figure 14.3 is a Scatchard plot of the saturation MsrA-ANS binding experiments. Experimental fluorescence values were normalized. For the linear transformation:

y-axis = [bound ANS]/[free ANS] = (ANS fluorescence emission)]/[ANS]
x-axis = [bound ANS] = (ANS fluorescence emission)

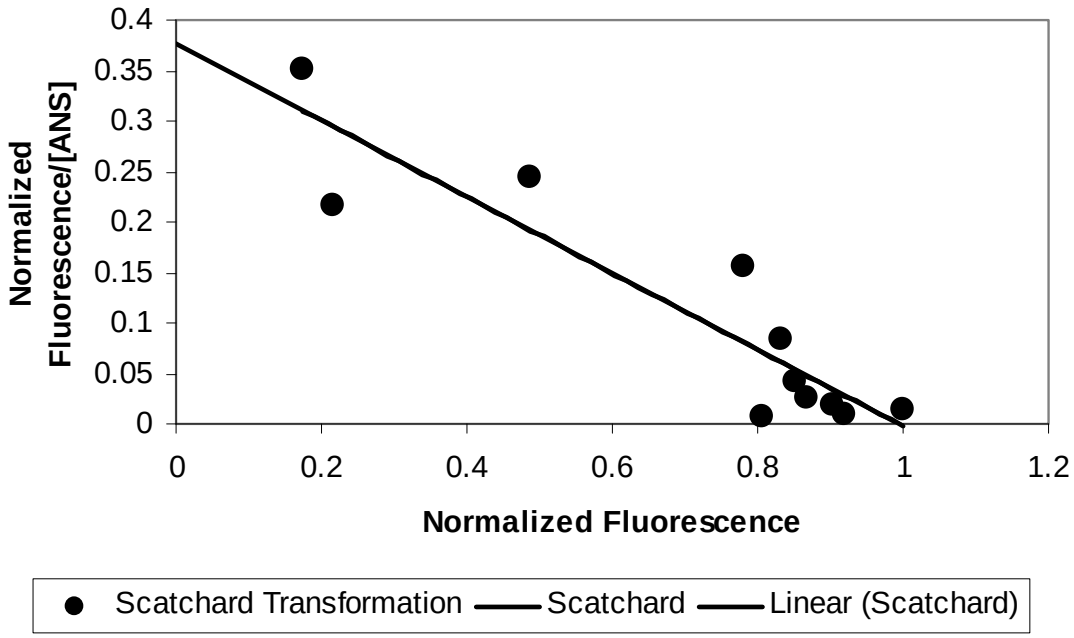

Figure 14.3. Scatchard transformation from MsrA-ANS saturation binding experiments. The data points are fit to a linear regression y=-0.379 + 0.376, R^2=0.842. x-intercept = 0.992.

The Scatchard linear regression has an x-intercept at 0.992, reporting that MsrA has one specific hydrophobic binding site.

Based on the primary sequence of MsrA, the Kyte-Doolittle hydropathy plot (Figure 5) defines the Cys-51 active site basin and its surrounding residues as the most hydrophobic region of MsrA. This solvent-exposed hydrophobic region is sterically accessible to ANS. This region is the hydrophobic binding site identified by using ANS.

Determination of Apparent K_d

Experimental evidence demonstrates that ANS is a ligand for MsrA and competes with other target ligands. This competition for interaction with MsrA suggests that there

exists a partioning of the equilibrium complex states. An apparent K_d of the affinity of MsrA for a specific target molecule may still be determined. The formation of complexes other than the specifically studied MsrA-target molecule is corrected for in the control experiments.

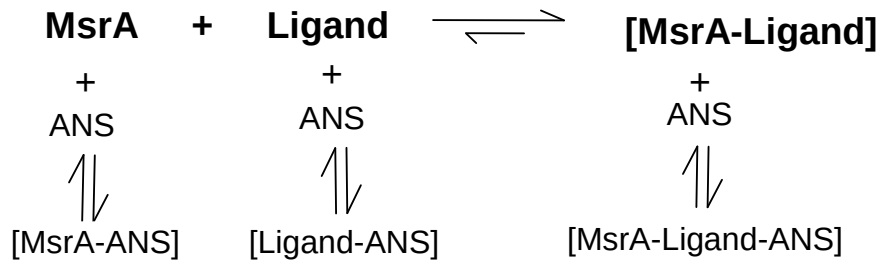

Figure 15. Schematic of free equilibrium species and complex formation.

Protein-ligand Interactions of MsrA, ANS, and Reduced Staph Nuclease Peptide

The exposure of hydrophobic regions and conformational changes in MsrA as the protein interacted with the reduced staph nuclease (SN) peptide was studied by peptide saturation binding experiments. The reduced SN peptide was manually titrated into the sample cell for fluorescence measurements at concentrations ranging from 0 – 100 μM peptide. The concentration of ANS was held constant at a concentration of 15 μM—a fifteen-fold excess of MsrA. Figure 16.1 is a plot of the controls and uncorrected experiments for this data set. Figure 16.2 is the plot of the corrected ANS fluorescence emission at 420 nm which indicates hydrophobic surface changes in MsrA alone.

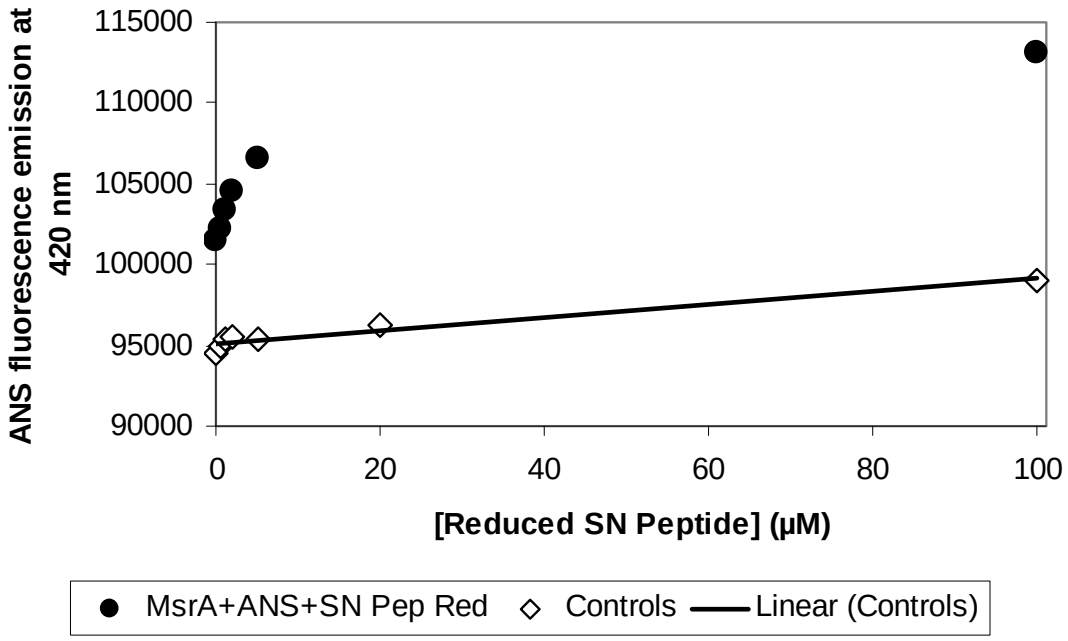

Figure 16.1. Experimental determination of change in exposed hydrophobic surface and apparent MsrA-reduced SN peptide dissociation constant. [ANS] = 15 µM.

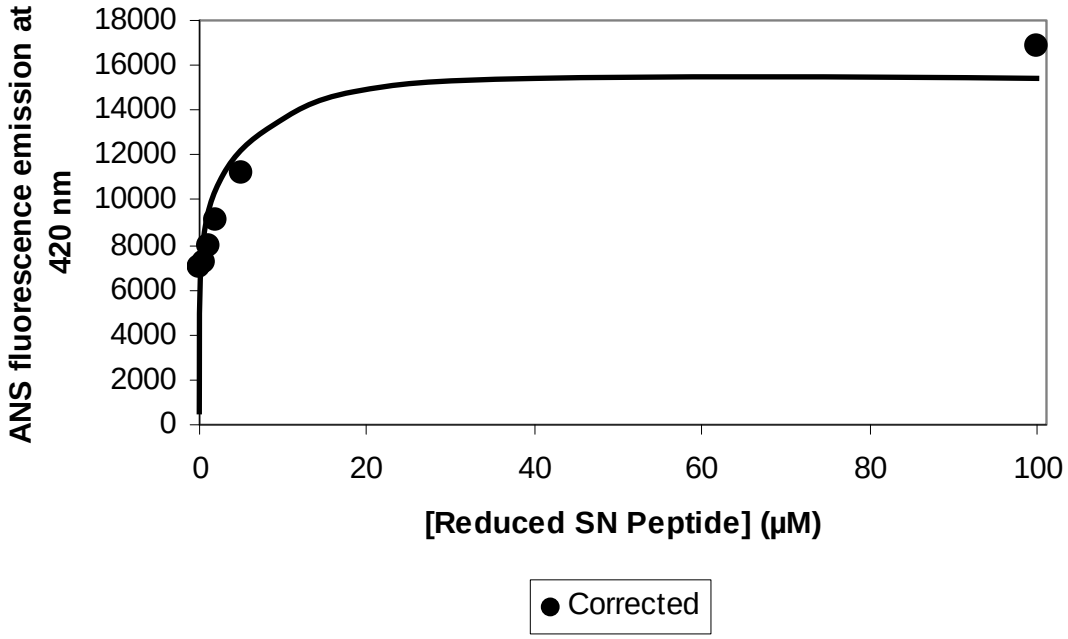

Figure 16.2. Corrected saturation binding curve for MsrA association with reduced SN peptide as reported by ANS. [ANS] = 15 µM.

The corrected ANS fluorescence emission results of this experiment reveals that MsrA interacts to some degree with the reduced peptide. Interestingly, this interaction results in an increase of exposed hydrophobic surface area of the MsrA-reduced SN peptide complex as reported by the increased fluorescence emission intensity. At 15 μM ANS, a ternary complex, comprised of MsrA, ANS, and the reduced peptide is formed. An apparent K_d of MsrA affinity for reduced SN peptide at [ANS] = 15 μM was determined to be 0.69 ± 0.64 μM.

With the reduced SN peptide as the target ligand, the experiment was performed at a greater ANS excess of 300 μM. This was to ensure that ANS was in sufficient excess of the maximum target molecule concentration and could still adequately report MsrA hydrophobic surface area changes for experiments in which very hydrophobic ligand interactions would be studied. The plot of this data is shown in Figure 16.3.

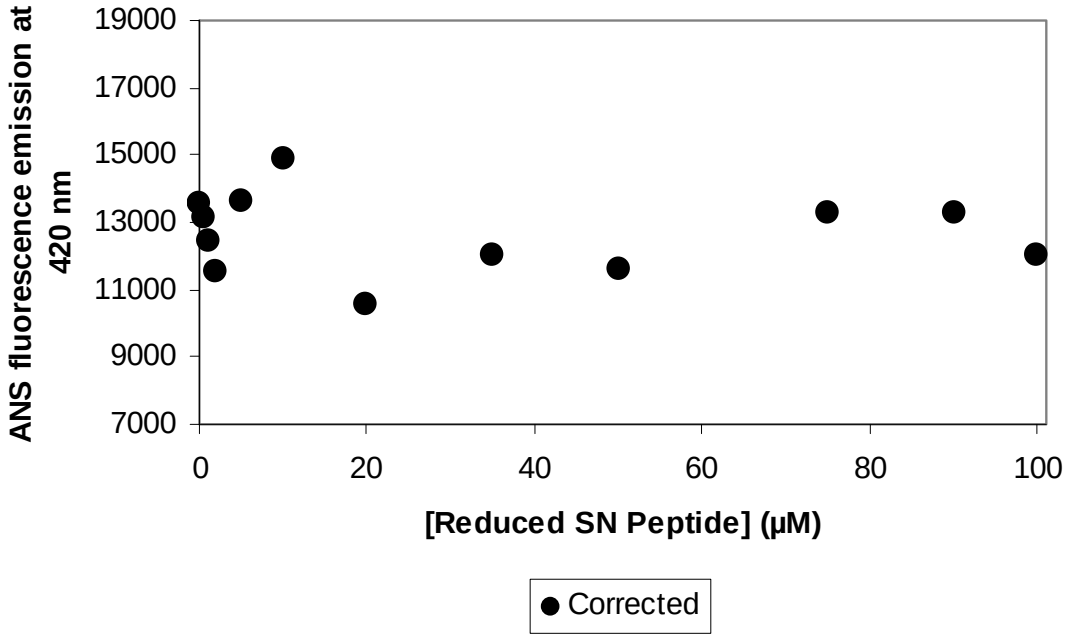

Figure 16.3. Corrected saturation binding data of MsrA binding affinity for the reduced SN peptide. [ANS] = 300 μM.

At [ANS] = 300 µM excess, the fluorescence emission of ANS displays no MsrA-reduced SN peptide saturation binding curve. The control and uncorrected experimental data plots were fit with a linear regression curve (Figure 16.4). Both curves have essentially the same slope. The increasing fluorescent intensity is a function of the only changing variable in both data sets: the increased peptide concentration due to titration. The ANS is in such excess that it completely and constantly occupies the hydrophobic binding site of MsrA and also binds to the hydrophobic surface of the peptide. As expected, the experimental data sample containing MsrA, ANS, and reduce SN peptide is offset at a higher fluorescent intensity since the experimental sample containing MsrA and peptide together have more hydrophobic surface area than the peptide alone.

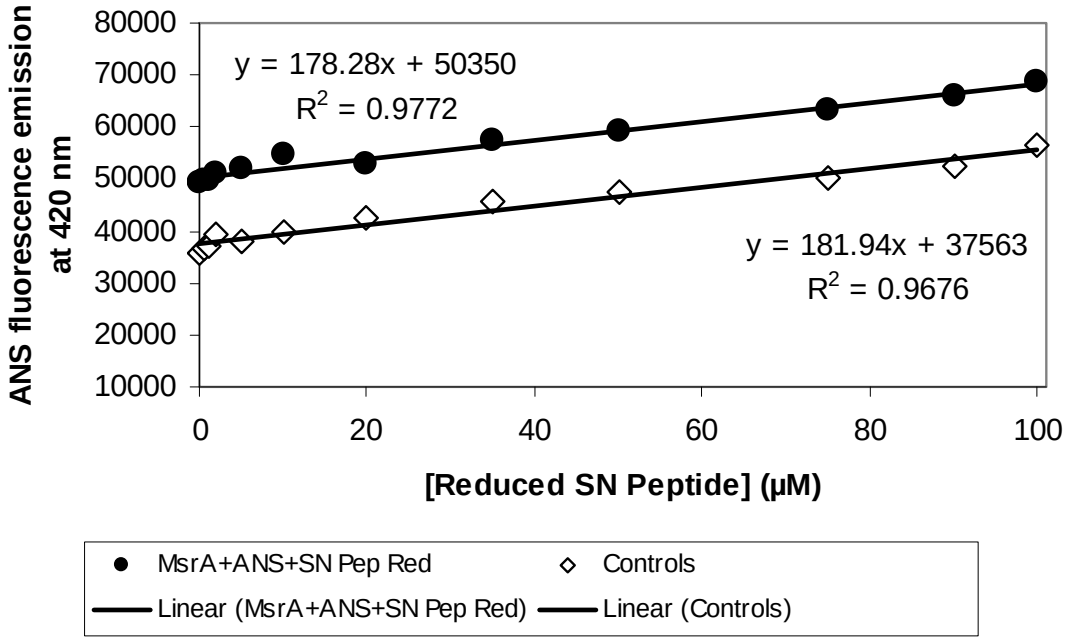

Figure 16.4. Uncorrected experimental fluorescence and control of MsrA with reduced SN peptide. [ANS] = 300 µM.

At the 300 µM ANS concentration, MsrA does not have a strong enough affinity for the reduced peptide. The reduced peptide cannot bind and displace ANS from the

hydrophobic active site. No dissociation hyperbolic curve could be derived from this data set. The corrected experimental data is simply a function of the difference in fluorescent emission of the ANS-reduced peptide complex in the presence and absence of MsrA and not strong MsrA-reduced peptide interactions.

Protein-ligand Interactions of MsrA, ANS, and Oxidized Staph Nuclease Peptide

Saturation binding curves for the MsrA-oxidized SN peptide were experimentally determined at constant ANS concentrations of 15, 100, and 300 µM. The data were fit by non-linear, hyperbolic decay regression curves. A persistent hyperbolic decrease in the fluorescence signal is reported in every experiment at each varying ANS concentration. Figures 17.1 – 17.6 show the plots of the uncorrected then corrected data from this set of equilibrium binding experiments.

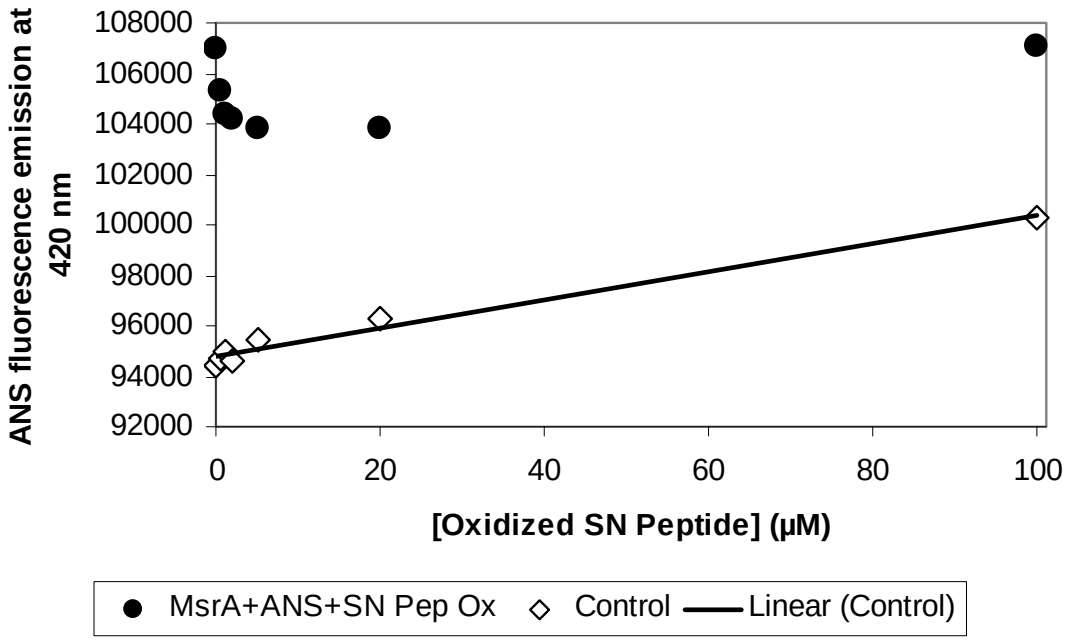

Figure 17.1. Saturation binding curve experiment of MsrA with oxidized SN peptide, uncorrected and control data. [ANS] = 15 µM.

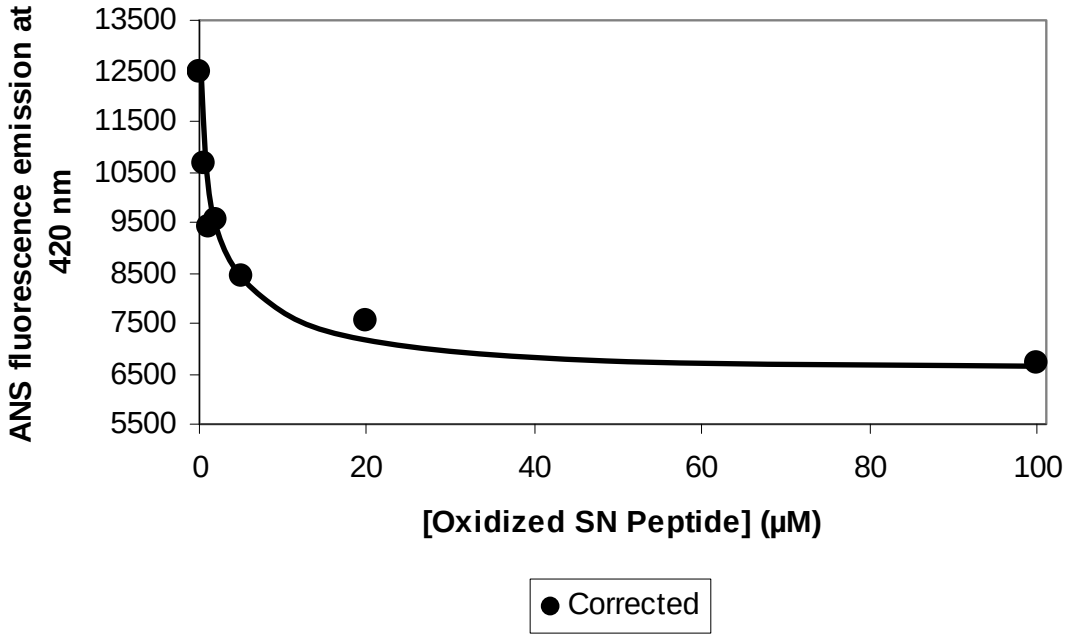

Figure 17.2. Corrected saturation binding curve of MsrA with oxidized SN peptide. [ANS] = 15 µM.

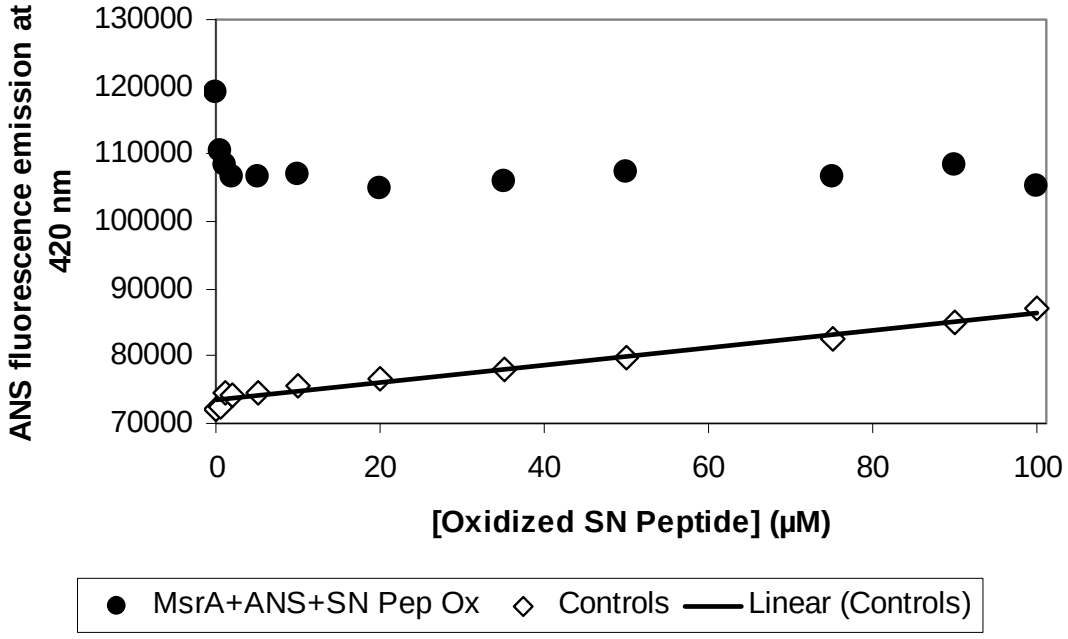

Figure 17.3. Saturation binding curve experiment of MsrA with oxidized SN peptide, uncorrected and control data. [ANS] = 100 µM.

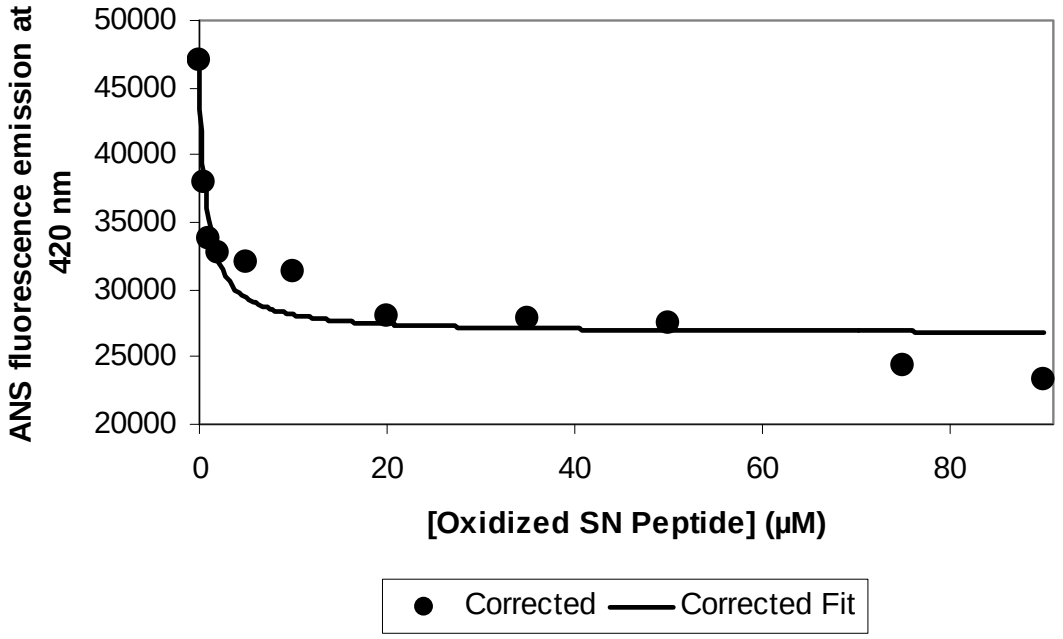

Figure 17.4. Corrected saturation binding curve of MsrA with oxidized SN peptide. [ANS] = 100 µM.

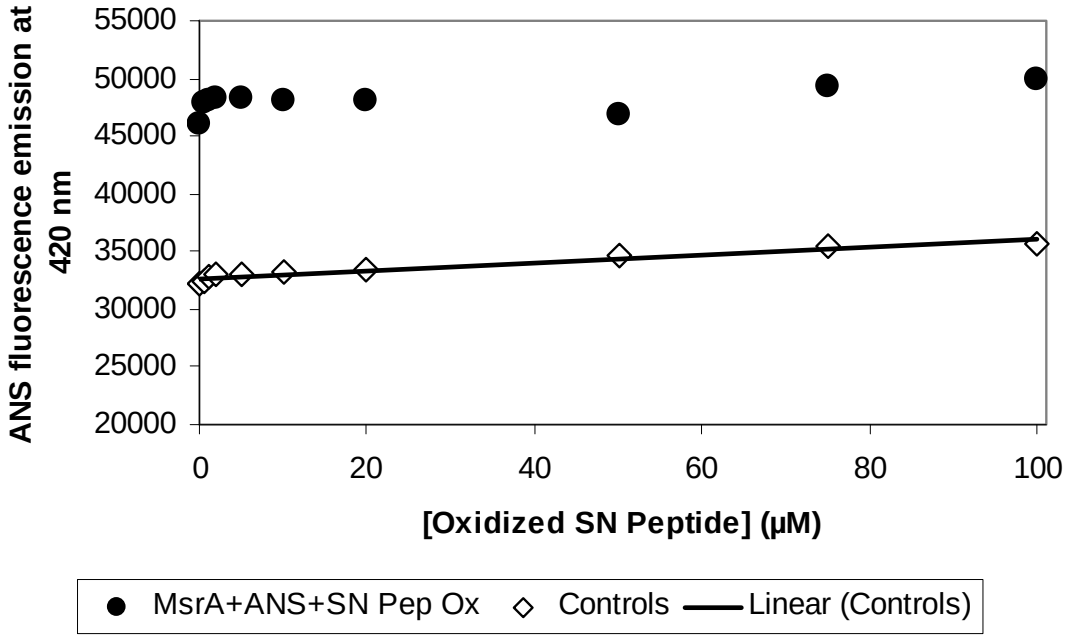

Figure 17.5. Saturation binding curve experiment of MsrA with oxidized SN peptide, uncorrected and control data. [ANS] = 300 µM.

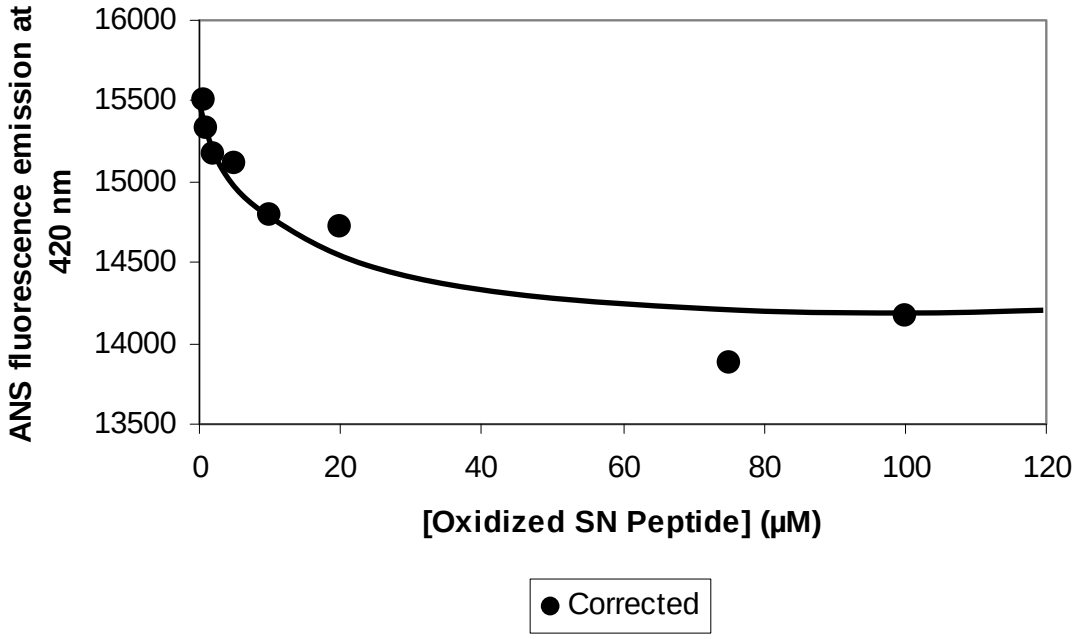

Figure 17.6. Corrected saturation binding curve of MsrA with oxidized SN peptide. [ANS] = 300 µM.

The apparent K_d's determined for the experiments with oxidized peptide were:

[ANS] (µM)	Apparent K_d (µM)
15	1.19 ± 0.41
100	0.78 ± 0.31
300	19.8 ± 10.0

The decay in the fluorescence signal was isolated to two possible causes: (1) as MsrA catalyzes the reduction of the sulfoxide, a conformational change occurs and the hydrophobic surface area of MsrA is buried, releasing ANS, or (2) that MsrA specifically has a higher affinity for the sulfoxide of the peptide, and ANS—which is stabilized on MsrA by weaker hydrophobic interactions—is displaced.

The catalytic repair mechanism of MsrA for oxidized substrates involves the formation of an intramolecular disulfide bond between Cys-51 and Cys-198. The distance between Cys-51 and Cys-198 is too large to allow the simple formation of an

intramolecular disulfide bond. As the MsrA active site binds a sulfoxide, MsrA undergoes a significant conformational change, bringing the otherwise distant Cys-198 close enough to Cys-51 to form the disulfide bond. During this conformational change, it was initially suspected that ANS may be displaced from its hydrophobic site on MsrA, or that hydrophobic sites on MsrA were buried and no longer solvent exposed.

As an oxidized substrate binds to MsrA, MsrA itself becomes oxidized ($MsrA_{Ox}$). Studies on the solved nuclear magnetic resonance (NMR) solution structures of wild-type $MsrA_{Ox}$ structure show the hydrophobic active site is more solvent exposed than the active site of the reduced form, displaying a hydrophobic patch on the molecular surface of MsrA (*16*). This increase in hydrophobic exposure allows the reductant thioredoxin to reduce MsrA back to its active state (Figure 4).

The three-dimensional spatial orientation of the atoms for these resolved solution structures (Protein Data Bank accession codes: 2gt3, reduced and 2iem, oxidized) (*17*) were analyzed using the program GETAREA™. GETAREA™ calculates the solvent-accessible surface area of biological macromolecules based on atomic spatial coordinates and local interactions with other atoms of the macromolecule. This data was used to determine the overall solvent-exposed surface area and hydrophobic (apolar) surface area of the oxidized versus the reduced form of MsrA (Table 3).

Table 3. MsrA Apolar Surface Area		
Model	**Apolar Area (Å²) $MsrA_{Ox}$**	**Apolar Area (Å²) $MsrA_{Red}$**
1	7441	6835
2	7583	6801
3	7823	6541
4	7351	6859
5	7826	6978
6	7717	7062
7	7328	6557
8	8128	6773
9	7986	6945
10	7745	6630
11	7663	6630
12	7576	6726
13	7476	6823
14	7827	6640
15	7653	6757
16	7757	6862
17	7543	6769
18	7704	6911
19	7822	6574
20	7476	6674

This data shows that the average exposed hydrophobic surface area of oxidized MsrA is greater (7671±162 Å²) than the exposed hydrophobic surface area of reduced MsrA (6767±117 Å²). The decreased fluorescence emission of ANS in the presence of oxidized peptide is therefore not a function of the burial of hydrophobic surface areas of MsrA upon repair of an oxidized substrate, but rather a competition reaction between ANS and the oxidized peptide for the MsrA Cys-51 active site region. The presence of the sulfoxide enhances MsrA substrate recognition and affinity such that ANS, even in great excess, was “outcompeted” for the active site. ANS could no longer bind with the occupied hydrophobic active site, falsely reporting a decrease in hydrophobic surface area as it was displaced from the complex.

Protein-ligand Interactions of MsrA, ANS, and Sulindac sulfide/Sulindac

Figure 18.1 shows the raw saturation binding curve data collected for the MsrA-sulindac sulfide experiment set. ANS is not expected to bind to sulindac sulfide, which contains no hydrophobic aminoacyl residues.

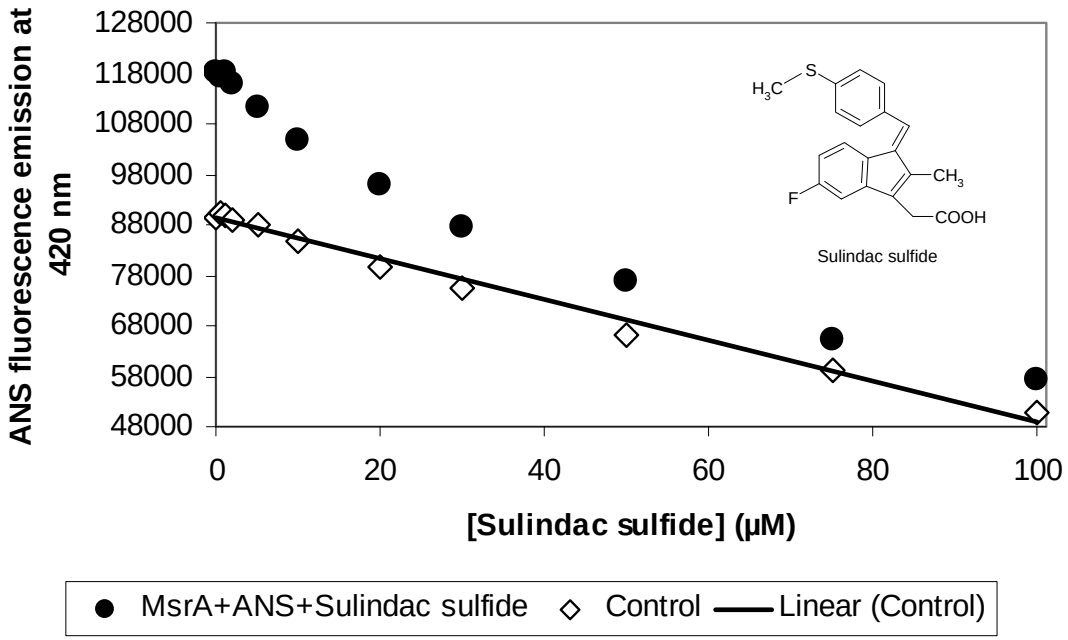

Figure 18.1. Saturation binding curve experiment of MsrA with sulindac sulfide, uncorrected and control data. [ANS] = 15 µM.

Interestingly, the control data shows that with increasing sulindac sulfide concentration the fluorescence emission intensity of ANS decreases considerably rather than remaining relatively constant. The same phenomenon is observed with the control data for sulindac shown in Figure 18.2.

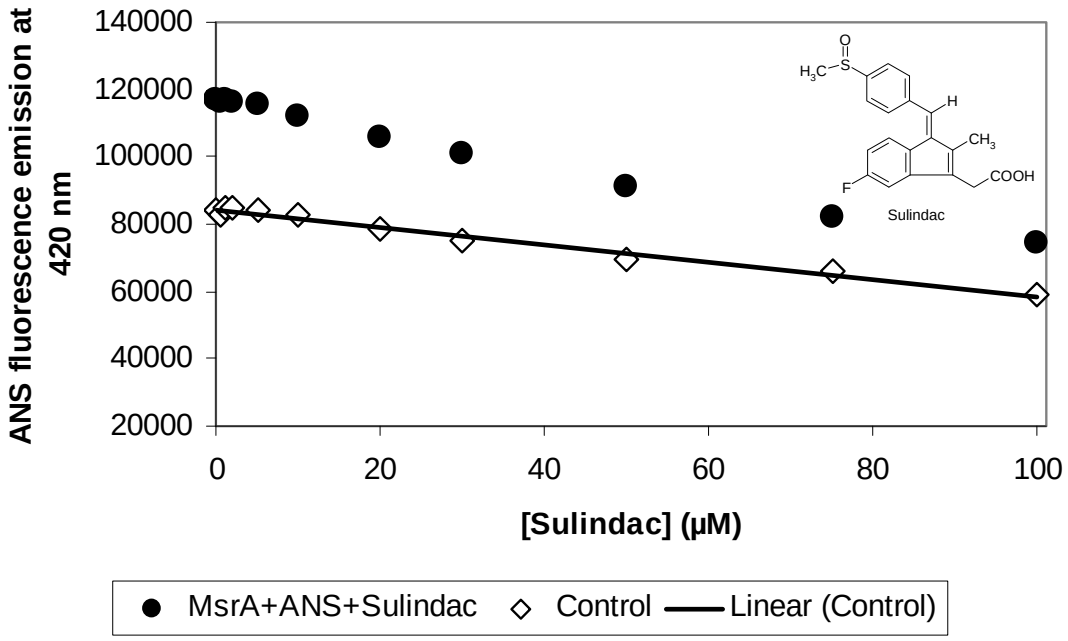

Figure 18.2. Saturation binding curve experiment of MsrA with sulindac, uncorrected and control data. [ANS] = 15 μM.

Sulindac and sulindac sulfide are both yellow, hydrophobic molecules. Perceived color is a function of the wavelength of light a molecule reflects while strongly absorbing the wavelength of light of the complementary color.

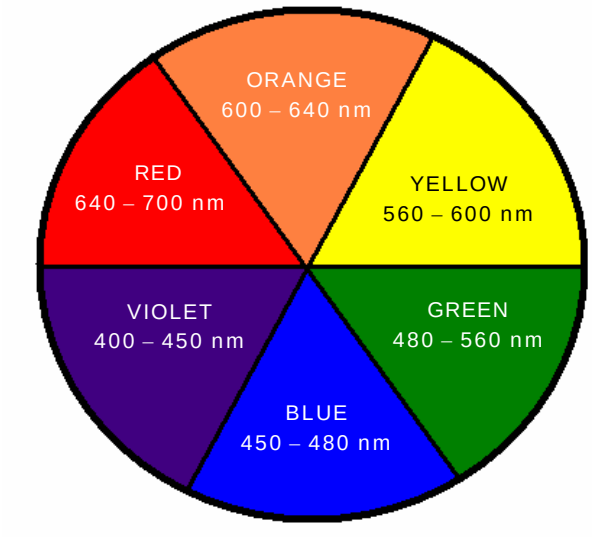

Figure 18.3. The complementary color wheel.

Figure 18.3 illustrates a color wheel, demonstrating the approximate wavelength absorbance relationships between complementary colors (*19*). Yellow compounds such as sulindac and sulindac sulfide theoretically strongly absorb violet visible light, 400 – 450 nm in wavelength.

The UV-vis absorbance spectrum of 50 µM sulindac in PBS (Figure 18.4) shows a local maximum peak at 328 nm from a scan range of 270 – 470 nm.

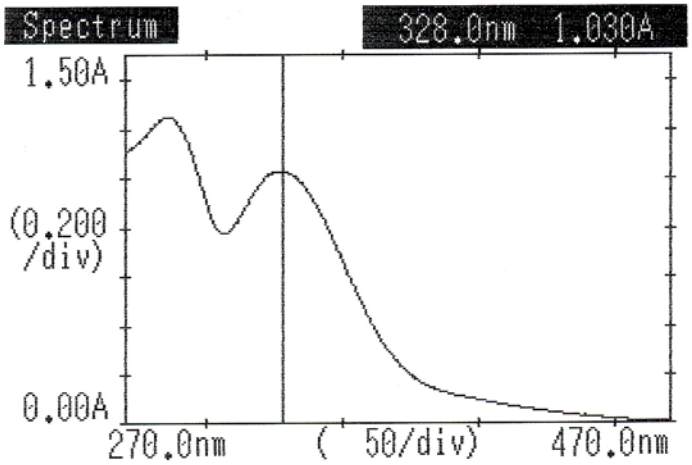

Figure 18.4. UV-vis absorbance spectrum of 50 µM sulindac in PBS.

Sulindac is shown to absorb light (0.058 absorbance units, A) of 420 nm in wavelength. This is the same wavelength of the monitored fluorescence emission of aminoacyl surface-bound ANS. This verifies that sulindac and sulindac sulfide quench the observed ANS fluorescence emission, resulting in the decreased fluorescence signal of the control data.

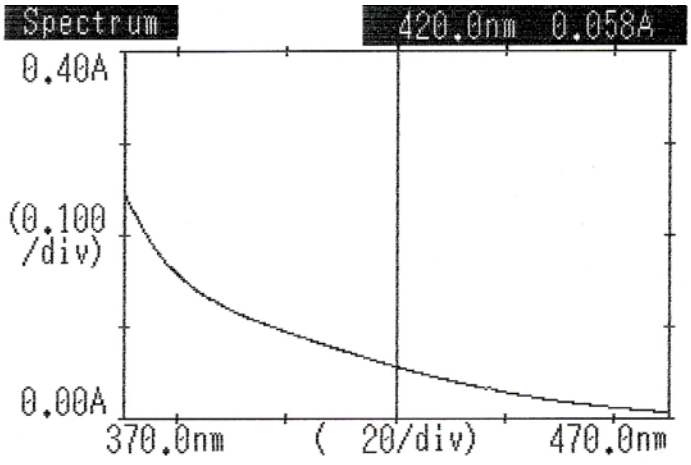

Figure 18.5. UV-vis absorbance spectrum of 50 µM sulindac in PBS at 420 nm.

Sulindac also absorbs light of 370 nm (Figure 18.6), the experimental excitation wavelength for ANS (Figure 18.6).

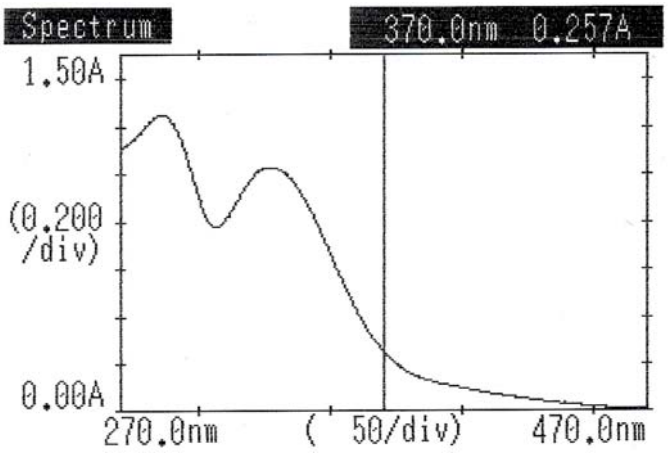

Figure 18.6. UV-vis absorbance of 50 µM sulindac in PBS at 370 nm.

At 370 nm, the absorption of ANS (0.267 A, Figure 18.7) is only slightly greater than the absorbance of sulindac (0.257 A) at the same concentration. This suggests that the decrease in ANS fluorescence with increasing sulindac/sulindac sulfide concentration is more greatly affected by the excitation light absorbed by sulindac/sulindac sulfide than the absorption of the ANS fluorescence emission wavelength at 420 nm. The absorption of the 370 nm excitation wavelength by sulindac/sulindac sulfide results in a diminished excitation energy delivered to ANS.

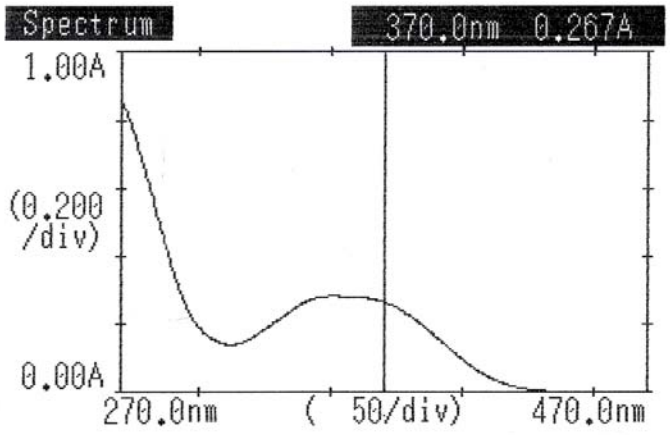

Figure 18.7. UV-vis absorbance of 50 µM ANS in PBS at 370 nm.

In summary, sulindac and sulindac sulfide competitively absorb the ANS excitation wavelength and quench the fluorescence emission of ANS at 420 nm as well. This results in the decreased fluorescence emission of ANS with increasing sulindac/sulindac sulfide concentration. The extinction coefficients of these species must be determined under these experimental conditions to more specifically address the strength of the absolute absorbance of ANS and sulindac/sulindac sulfide.

Despite the relative quenching factor, the hyperbolic decay trend for the uncorrected and corrected (Figures 18.8 and 18.9) experimental data for the MsrA interaction with sulindac sulfide and sulindac suggests that the greater MsrA affinity for the two species is real. Sulindac and sulindac sulfide displace ANS from the MsrA active site. What is most noteworthy is that even with the absence of a sulfoxide, sulindac sulfide is sufficiently hydrophobic and is able to displace ANS from the MsrA hydrophobic active site, resulting in the decreased ANS fluorescence emission.

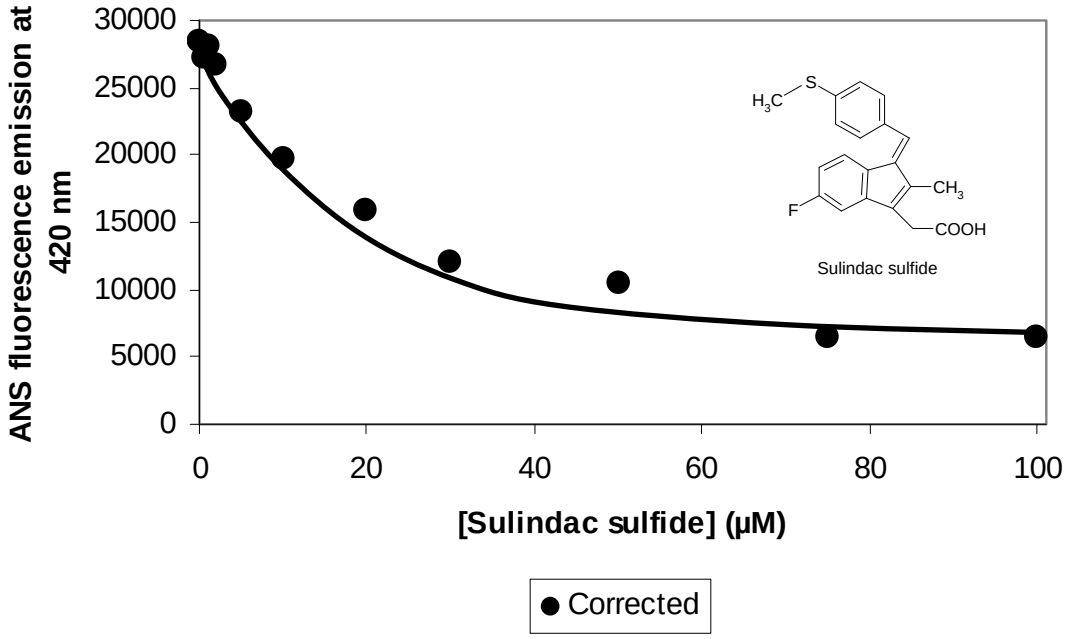

Figure 18.8. Corrected saturation binding curve experiment of MsrA with sulindac sulfide. [ANS] = 15 µM.

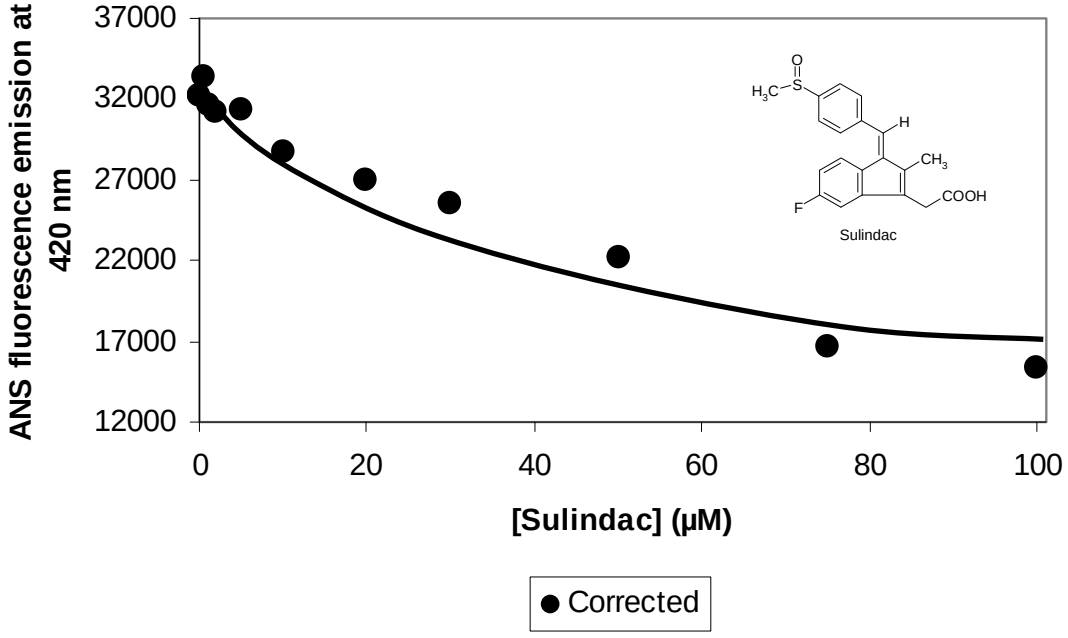

Figure 18.9. Corrected saturation binding curve experiment of MsrA with sulindac. [ANS] = 15 µM.

Ultimately, to minimize the effects of the sulindac/sulindac sulfide quenching phenomenon, it would be instructive to excite and monitor the fluorescence emission of ANS at a higher wavelength, where the absorbance of sulindac/sulindac sulfide is minimized.

Protein-ligand Interactions of MsrA, ANS, and Reduced Wild-type Staph Nuclease

The first documented recognition mechanism studies of MsrA for a full protein were investigated with wild-type staphylococcal nuclease (WT SN). The reduced form of WT SN is not a catalytic substrate for MsrA. As MsrA recognizes and interacts with the reduced ligand, the enzyme should not undergo significant conformational change nor proceed through its catalytic cycle. Figure 19.1 shows the raw experimental data of the MsrA interaction with reduced WT SN monitored at 15 μM ANS.

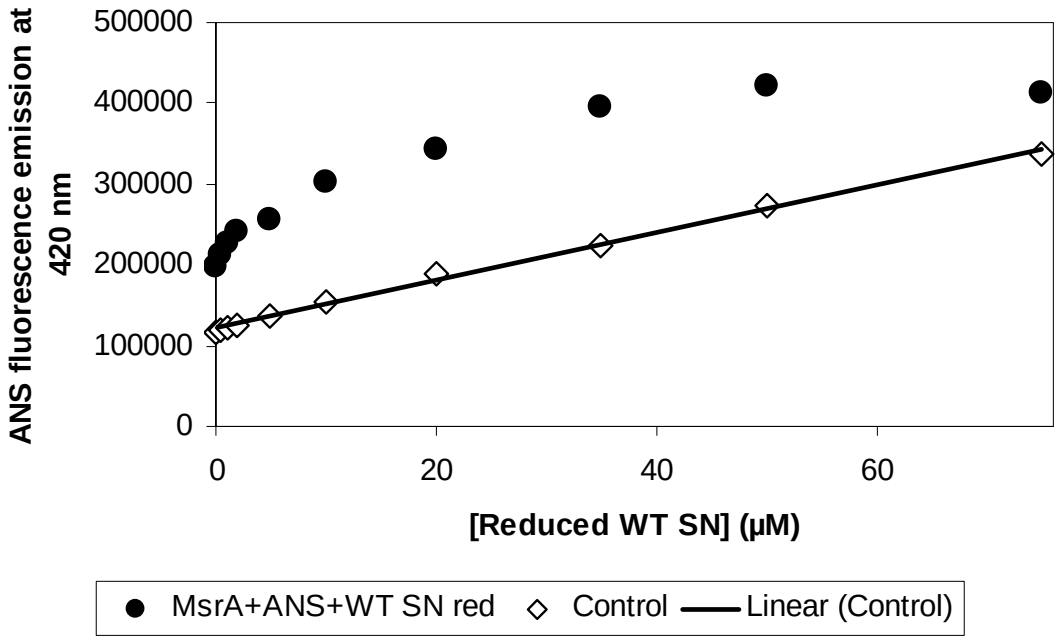

Figure 19.1. Saturation binding curve experiment of MsrA with reduced WT SN, uncorrected and control data. [ANS] = 15 μM.

The corrected data for this experiment (Figure 19.2) shows an initial increase of the ANS fluorescence emission signal, then a signal intensity decline beginning at a concentration of approximately 35 μM WT SN.

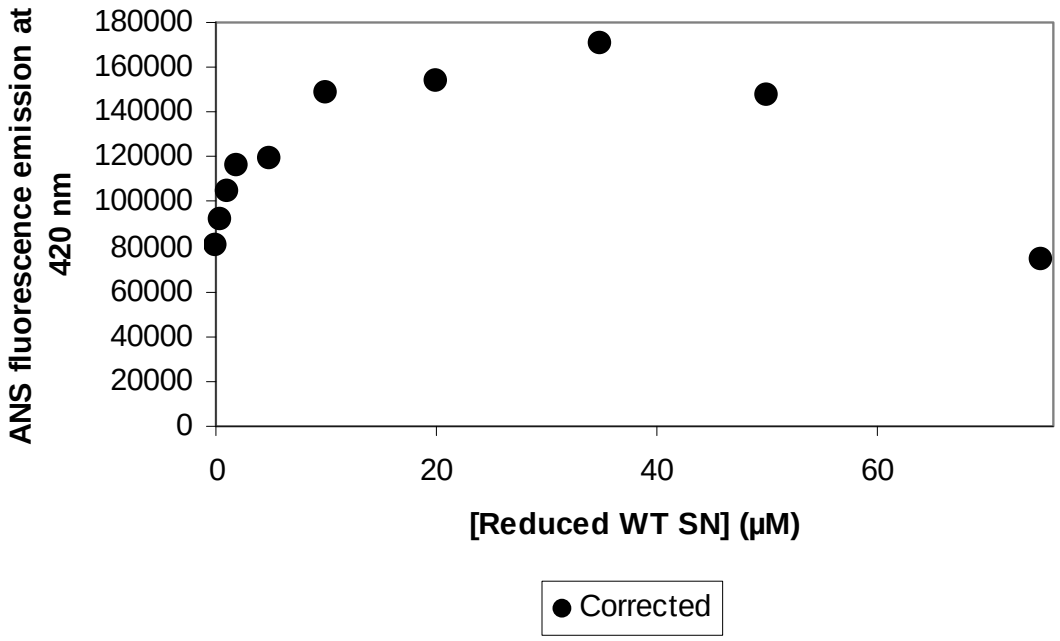

Figure 19.2. Corrected saturation binding curve experiment of MsrA with reduced WT SN. [ANS] = 15 µM.

In this experiment, at approximately 35 µM WT SN, the observed fluorescence decrease results as the equilibrium reaction shifts to favor the formation of the bi-molecular complex of MsrA and reduced WT SN, displacing ANS.

Figure 19.3 is the raw data for the MsrA-WT SN equilibrium interaction at [ANS] = 100 µM. Figure 19.4 shows that the same intensity increase is observed with the MsrA-WT SN equilibrium interaction at high ANS concentration, however, resulting in a maximum saturation intensity rather than eventual decay.

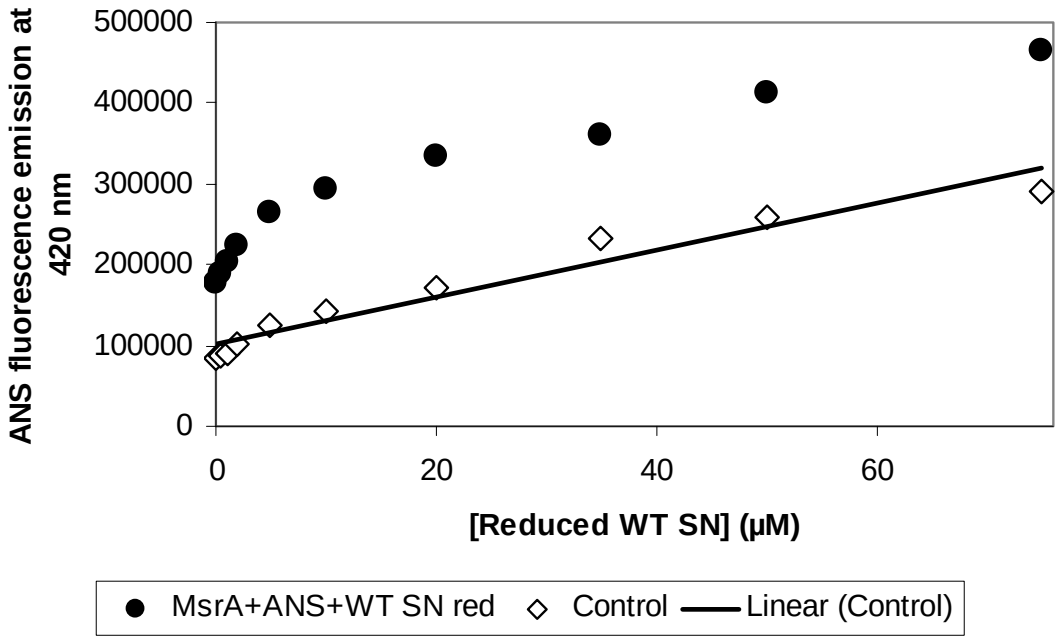

Figure 19.3. Saturation binding curve experiment of MsrA with reduced WT SN, uncorrected and control data. [ANS] = 100 µM.

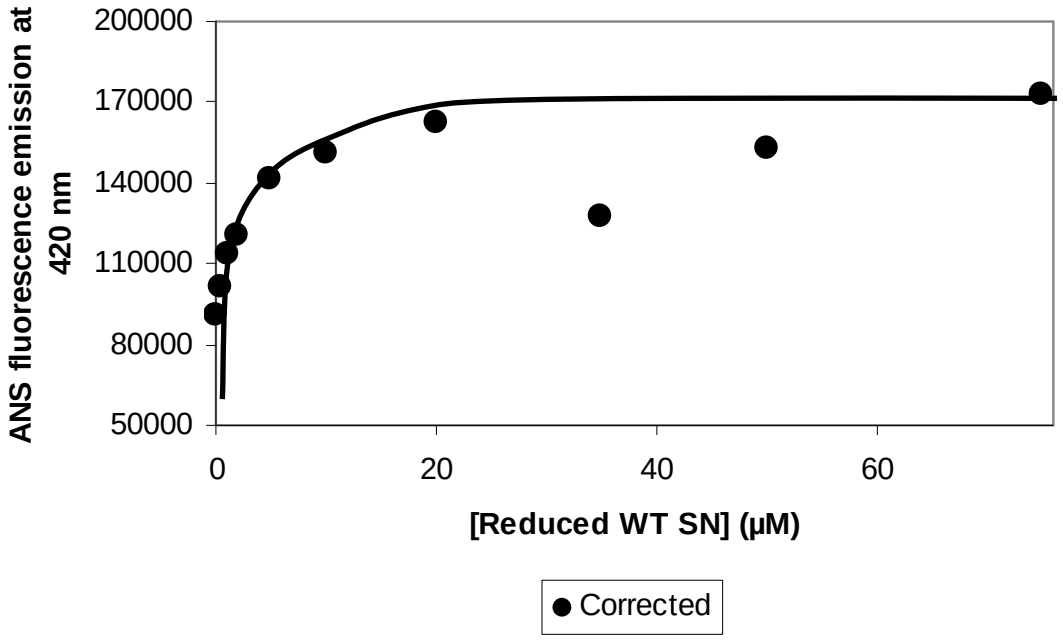

Figure 19.4. Corrected saturation binding curve experiment of MsrA with reduced WT SN. [ANS] = 100 µM.

The initial increase in ANS fluorescence emission with increasing WT SN at high and low ANS concentrations is the same trend observed from the MsrA interaction with the reduced SN peptide at low ANS concentration. These experiments support the notion that the presence of the reduced ligands in increasing concentration encourages ANS accessibility to the MsrA hydrophobic binding site, forming a ternary complex at equilibrium and resulting in a greater signal intensity.

It can be argued that the displacement of ANS from MsrA at [ANS] = 15 μM is artificially forced by the increased WT SN titration resulting in increased molecular collisions between the proteins rather than a specific hydrophobic affinity effect. Data from experiments with SN T62P, however, strongly supports the latter.

Protein-ligand Interactions of MsrA, ANS, and Reduced Staph Nuclease T62P

The site-directed mutagenesis of Thr-62 replaced with proline in wild-type staph nuclease results in the formation of SN T62P, a natively unstructured, extremely hydrophobic molecule. The equilibrium of interaction of MsrA with reduced SN T62P in the presence of 15 µM ANS is shown in Figures 20.1 and 20.2.

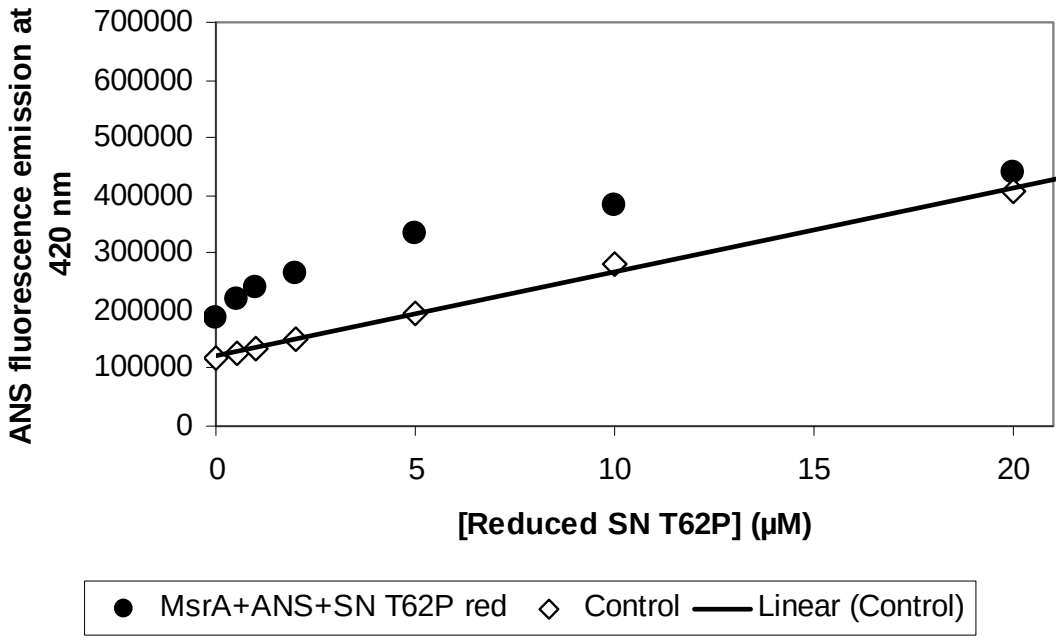

Figure 20.1. Saturation binding curve experiment of MsrA with reduced SN T62P, uncorrected and control data. [ANS] = 15 µM.

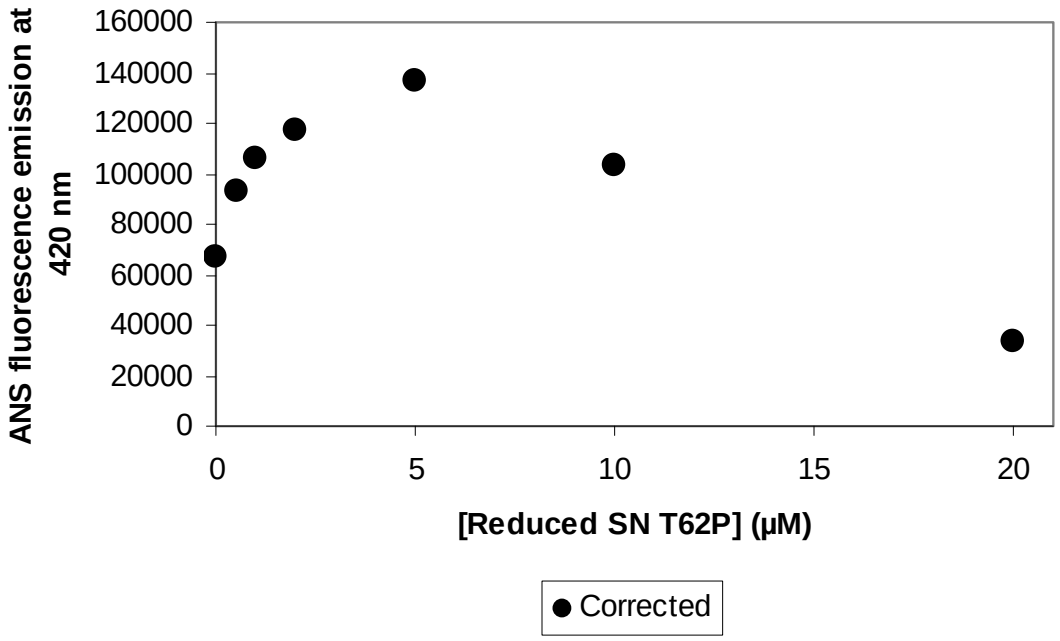

Figure 20.2. Saturation binding curve experiment of MsrA with reduced SN T62P, uncorrected and control data. [ANS] = 15 μM.

The corrected experimental data of the MsrA interaction with reduced SN T62P shows an initial hyperbolic increase in the ANS fluorescence signal. At 5 μM SN T62P, there begins a marked decrease in the ANS fluorescence emission suggesting the favored formation of the bi-molecular MsrA-SN T62P complex. Most notably, this complex formation is favored at a lower SN T62P (5 μM) concentration than WT SN (35 μM) at the same ANS concentration. This further supports the theory of a specific hydrophobic affinity of MsrA for its target substrates since WT SN and SN T62P differ only by one modified residue resulting in significant structural disruption and ultimately increased protein hydrophobicity.

Conclusions

Oxidative modification of biological molecules has significant implications for the propagation and pathology of neurodegenerative disease and aging. The enzyme methionine sulfoxide reductase A is capable of specifically reversing oxidative modification to methionine of a wide range of biological and non-biological molecules. We studied the recognition mechanism of MsrA—how MsrA is able to recognize and reduce sulfoxides on many ligands. Physiologically, biological macromolecules randomly interact with various ligands by weak van der Waals forces or hydrophobic interactions. Substrate recognition specificity is determined by: (1) the structural and chemical properties of the enzyme of interest and (2) the features of each target molecule that optimize binding affinity.

Structural studies of MsrA show that the enzyme active site is a solvent exposed hydrophobic pocket. Kyte-Doolittle hydropathy analysis shows that the active site region is the most hydrophobic surface of MsrA. We specifically investigated the hydrophobic interactions of MsrA with its ligands since proteins damaged by oxidative modifications become misfolded, often resulting in exposure of normally-buried hydrophobic regions.

We studied the propensity of MsrA to form complexes with four specific, biological and non-biological ligands. We used the fluorophore 8-anilino-1-naphthalene sulfonic acid (ANS) as a reporter for the exposure or burial of hydrophobic surfaces on MsrA as the enzyme interacted with the ligands. Beyond providing information on structural changes of the enzyme, ANS was itself a hydrophobic ligand for the active site of MsrA and competed with the initially chosen target molecules for binding.

These studies provided information on the dissociation constant of the MsrA-ANS

complex and apparent dissociation constants of the complexes formed by MsrA and the original target molecules. By a series of saturation binding curve experiments of MsrA and ANS, the Cys-51 active site pocket was isolated as the single, unique hydrophobic binding site. ANS ultimately served as a reporter for the relative affinity of MsrA for the other target molecules in the ligand competing experiments.

From these competing reactions, we determined that the reduced form of a peptide derived from the first α-helix of the full protein staphylococcal nuclease enhances the exposure of hydrophobic surfaces on MsrA, forming a ternary complex of MsrA, reduced SN peptide, and ANS. At high ANS concentrations, this reduced peptide could not successfully compete for the hydrophobic active site of MsrA. At low and high ANS concentrations however, the oxidized form of the same peptide actively competed for the MsrA active site, displacing ANS.

MsrA equilibrium binding experiments with the non-protein molecules sulindac and sulindac sulfide both showed a hyperbolic decay of the fluorescence emission intensity of ANS with increasing sulindac/sulindac sulfide concentration. Of note, these studies showed that MsrA preferentially binds sulindac sulfide over ANS, despite the absence of a sulfoxide or charged residue.

We extended the investigation into the first studies of the recognition and affinity of MsrA for full protein ligands. The presence of the reduced form of wild-type staphylococcal nuclease (WT SN) and staph nuclease T62P (SN T62P) at low concentrations causes an increased exposure of hydrophobic surface area on MsrA, resulting in the formation of a ternary complex comprised of MsrA, ANS, and the staph nuclease protein. With increased titrated staph nuclease (WT and T62P) concentration,

however, ANS is outcompeted for occupation of the hydrophobic MsrA active site. Most notably, this complex formation is favored at a lower SN T62P concentration than WT SN. SN T62P differs from WT SN by only one mutated residue which results in severe structural disruption and increased exposed hydrophobic surface area of the protein. It is significant that MsrA interacts with these reduced proteins, in spite of the absence of sulfoxide modifications.

The increased affinity of MsrA for the hydrophobic protein SN T62P strongly supports the hypothesis that MsrA functions as a chaperone. That is, MsrA recognizes misfolded proteins nonspecifically based on exposed hydrophobic regions then specifically repairs methionine sulfoxide modifications that may have produced the misfolded structure. With this research we have demonstrated an MsrA target molecule recognition mechanism of weak, but specific hydrophobic interactions enhanced by the presence of a sulfoxide. The work described above represents the first investigations of the interaction of MsrA with physiologically relevant ligands and has laid the foundation for a novel method of investigating the hydrophobic recognition mechanism of MsrA as a chaperone for oxidatively modified target molecules.

Future Work

- Further characterize the forces that stabilize MsrA-ligand interaction by isothermal titration calorimetry experiments to derive thermodynamic association constants such as the stoichiometry of interaction, heat capacity of binding, entropy, enthalpy, and free energy of the MsrA-ligand binding.
- Investigate the role of specific residues of the MsrA active site by manipulating the hydrophobicity/hydrophilicity of the active site residues by site-directed mutagenesis.
- Investigate the role of the long, flexible hydrophobic N-terminus coil (Ser-1 through Met-42) in the possible stabilization of large protein ligands at the MsrA active site.
    - Perform ligand interaction experiments with a mutated form of MsrA where the N-terminus is truncated.
- Obtain a crystal structure of MsrA with ligand bound in the active site.

References

1. Tete-Favier, F., Cobessi, D., Boschi-Muller, S., Azza, S., Branlant, G., Aubry, A. (2000). Crystal structure of the *Escherichia coli* peptide methionine sulphoxide reductase at 1.9 Å resolution. *Struct. Fold. Des. 8:* 1167 – 1178.
2. Brot, N., Weissbach, H. (2000). Peptide methionine sulfoxide reductase: Biochemistry and physiological role. *Peptide Sci. 55:* 288 – 296.
3. Weissbach, H., Resnick, L., Brot., N. (2004). Methionine sulfoxide reductases: History and cellular role in protecting against oxidative damage. *Biochi. Biophy. Acta. (BBA)1703(2):* 203 – 212.
4. Singh, V., Moskovitz, J. (2003). Multiple methionine sulfoxide reductase genes in *Staphylococcal aureus*: expression of activity and roles in tolerance of oxidative stress. *Microbiology 149:* 62 – 65.
5. Wizeman, T.M., Moskovitz, J., Pearce, B.J., Cundell D. (1996). Peptide methionine sulfoxide reductase contributes to the maintenance of adhesins in three major pathogens. *Proc. Natl. Acad. Sci. USA 93(15):* 7985-7987.
6. Volkin, D.B., Mach, H. and Middaugh, C.R. (1997). *Mol. Biotech. 8:* 105 – 122.
7. Kim, Y.H., Berry, A.H., Spencer, D.S., Stites, W.E. Comparing the effect on protein stability of methionine oxidation versus mutagenesis: steps toward engineering oxidative resistance in protein. *Prot. Eng. 14(5):* 343 – 347.
8. Kuschel, L., Hansel, A., Schonherr, R., Weissbach, H., Brot, N., Hoshi, T., Heinemann, S.H. (1999). Molecular cloning and functional expression of a human peptide methionine sulfoxide reductase (hMsrA). *FEBS Lett 56:* 17 – 21.
9. DeLano, W.L. "The PyMOL Molecular Graphics System." DeLano Scientific LLC, San Carlos, CA. *Electronic references:* http://www.pymol.org. Accessed January 17, 2007.
10. Lowther, W.T., Brot, N., Weissbach, H., Matthews, B.W. (2000). Thiol-disulfide exchange is involved in the catalytic mechanism of peptide methionine sulfoxide reductase. *Proc. Natl. Acad. Sci. USA 97:* 6463 – 6468.
11. Gasteiger, E., Hoogland, C., Gattiker, A., Duvaud, S., Wilkins, M.R., Appel, R.D., Bairoch, A. (1999). Protein identification and analysis tools on the ExPASy server. *Methods Mol. Biol. 112:* 531-552.
12. Chen, J., Lu, Z., Sakon, J., Stites, W.E. (2000). Increasing the thermostability of staphylococcal nuclease: implications for the origin of protein thermostability. *J.Mol.Biol. 303:* 125-130.
13. Diamond, D., Randall, L.; Kinetic Partitioning: Poising SecB to Favor Association with a Rapidly Folding Ligand (1997). *J. Biol. Chem. 272(46*): 28994-28998.
14. Muñoz, V., Serrano, L. (1994). Elucidating the folding problem of a-helical peptides using empirical parameters, II. Helix macrodipole effects and rational modification of the helical content of natural peptides. *J. Mol. Biol 245:* 275-296.
15. Motulsky, H., Christopoulos, A. (2003). "Fitting Models to Biological Data using Linear and Nonlinear regression." San Diego, CA. *Electronic references:* www.curvefit.com/scatchard_plots.htm. Accessed April 12, 2008.
16. Coudevylle, N., Antoine, M., Bouguet-Bonnet, S., Mutzenhardt, P., Boschi-Muller, S., Branlant, G., Cung, M. (2007). Solution structure and backbone dynamics of the reduced form and an oxidized form of *E. coli* methionine sulfoxide reductase A (MsrA):

structural insight of the MsrA catalytic cycle. *J. Mol. Biol. 366:* 193 – 206.
17. Berman, H.M., Westbrook, J., Feng, Z., Gilliland, G., Bhat, T.N., Weissig, H., Shindyalov, I.N., Bourne, P.E. (2000). The Protein Data Bank. *Nucleic Acids Research 28:* 235-242.
18. Fraczkiewicz, R; Braun, W. (1998). Exact and efficient analytical calculation of the accessible surface areas and their gradients for macromolecules. *J. Comp. Chem. 19:* 319- 333.
19. Dartmouth College (2007). "ChemLab: Color and Light." Hanover, NH *Electronic references:* http://www.dartmouth.edu/~chemlab/chem6/dyes/full_text/chemistry.html. Accessed April 28, 2008.

APPENDIX I
Definitions and Notations

Active site	the part of an enzyme where a target molecule binds
Adhesin	filamentous protein structure on the surface of bacteria that allow bacteria to adhere to a host organism
Aggregation	the tendency of damaged proteins to clump together
Anti-oxidant	a molecule that is capable of slowing or preventing the oxidation of other molecules
Amino acid	a molecule that is the basic building block of proteins
Chaperone	a class of proteins that recognize features of unfolded proteins and function to prevent improper associations between proteins
Cysteine	a naturally occurring sulfur-containing amino acid
Denature	altering the structure of a protein by some sort of stress (i.e. heat or change in pH) so that the protein can no longer function
Enantiomers	a pair of molecules that have the same molecular formula but are structurally non-superimposable mirror images of each other
Enzyme	a class of proteins that accelerate chemical reaction rates
Eukaryote	a single or multi-celled organism whose cells contain a nucleus enclosing the cell's genetic material
Functional group	a specific group of atoms within a molecule that is responsible for the characteristic chemical reactions of that molecule
Extrinsic fluorescence	inherent fluorescence of external molecular probes
Hydrophilic	water loving; polar
Hydrophobic	water fearing; nonpolar
Kinetics of association	the rates at which a protein recognizes its target molecule

Knockout	also referred to as "gene knockout," the process of genetically engineering an organism to make a gene inoperative, or non-functional
Monomeric protein	a protein containing a single subunit
Ligand	a target molecule that binds to with a larger molecule
Methionine	a sulfur containing amino acid
Mutagenesis	the process of mutating a target molecule; in the context of proteins, mutagenesis refers to the substitution of one amino acid for another at a specific position
Native structure	the functional form/three-dimensional structure of a protein
Oxidation	the process of combining oxygen with some other substance; a chemical change in which an atom loses electrons
Peptide	a short chain of amino acids
Polymer	a large molecule comprised of linked series of structural units
Protein	a linear polymer made of combinations of the 20 amino acids
Reagent (Reactant)	an agent that serves as a starting material in a chemical reaction
Recognition mechanism	the means by which a protein, specifically an enzyme, is able to recognize its target molecule
Recombinant DNA	a form of genetic engineering whereby two strands of DNA that do not normally occur together are artificially combined (combination of DNA that codes for MsrA and GST to form the MsrA-GST fusion protein)
Reducing agent	the compound in a reaction that reduces another compound as it becomes oxidized itself
Reduction	any process in which electrons are added to an atom or ion (as by removing oxygen)
Residue	in protein biochemistry, a residue refers to an amino acid

Side chain	a molecule that is attached to a core structure; in proteins, an amino acid
Stoichiometry	the proportions of reactants and products in a chemical reaction
Substrate	a target molecule that is enzymatically modified
Tryptophan	an aromatic amino acid that has intrinsic fluorescence
Tyrosine	an aromatic amino acid that has intrinsic fluorescence

APPENDIX II
Amino Acid Letter Codes

Amino Acid	1-letter Code	3-letter Code
Alanine	A	Ala
Arginine	R	Arg
Aspargine	N	Asn
Aspartic acid	D	Asp
Cysteine	C	Cys
Glutamic acid	E	Glu
Glutamine	Q	Gln
Glycine	G	Gly
Histidine	H	His
Isoleucine	I	Ile
Leucine	L	Leu
Lysine	K	Lys
Methionine	M	Met
Phenylalanine	F	Phe
Proline	P	Pro
Serine	S	Ser
Threonine	T	Thr
Tryptophan	W	Trp
Tyrosine	Y	Tyr
Valine	V	Val

APPENDIX III
MsrA Growth and Purification Protocol

Growth of *E.coli* BL21-DE3 for the Overexpression of MsrA

BL21-DE3 *E.coli* cells selected for the overproduction and isolation of MsrA were grown on a luria broth agar plate with an ampicillin concentration of 50μg/mL. MsrA in these cells exists as a recombinant glutathione-S-transferase (GST) fusion protein which can be purified by affinity techniques using an immobilized glutathione column without potential for the denaturation of the protein. Ten *E.coli* colonies were isolated and inoculated into small scale 2 mL luria broth volumes of 50μg/mL ampicillin (LB-amp_{50}) and grown overnight. The growth scale was progressively increased in 100 mL volumes of LB-amp_{50} then ultimately to two 700 mL volumes of LB-amp_{50}. The cells were grown to an optical density at 600 nm (OD_{600}) of approximately 0.750. At this optical density, the *lac*-inducer isopropyl β-D-1-thiogalactopyranoside (IPTG) was added to the large scale volumes to produce a final 0.5mM concentration of IPTG to signal the cells to commence protein overexpression. The cultures were grown for two more hours. The cells were harvested by centrifugation then stored at -80°C.

Isolation and Purification of MsrA

The BL21-DE3 cell pellets were lysed using phosphate buffered Bacterial Protein Extraction Reagent (BPER) from Pierce™. BPER is a proprietary lysing solution based on a nonionic detergent that disrupts the cell membrane allowing the intracellular contents to be released. The lysate supernatant was removed and filtered and the pellet was discarded. The cell lysate was loaded onto the GSTPrep™ Fast-Flow 16/10 column pre-packed with immobilized glutathione sepharose connected to the ÄKTAprime™ chromatographic system. Once loaded onto the column, the column was washed with

phosphate buffered saline (PBS), pH 7.3 and the protein content of the flow-through from the column was measured using an inline UV-vis absorbance detector set at 280 nm. The recombinant MsrA-GST fusion protein was eluted from the column using a solution of freshly prepared tris-glutathione, pH 8.0. The solution was exchanged into PBS by dialysis and the fusion protein was then cleaved using thrombin protease with shaking overnight at 4°C. Thrombin was removed by passing the solution over a benzamidine sepharose resin specifically binding thrombin alone yielding pure MsrA.

Induction Tests

To investigate the overproduction efficiency of the E.*coli* MsrA stocks, induction tests were performed on twenty randomly selected colonies. Small scale volumes of 2mL LB-amp$_{50}$ were inoculated and grown to OD ~0.75. Samples of each were saved to observe the pre-induction state of protein overexpression in the cells. IPTG was then added to a final concentration of 1mM. The cultures were grown for two more hours and samples of each were saved for comparison to the pre-induction protein production. Figure 21.1 is the SDS-PAGE analysis of five pre and post induction colonies. The bold band at ~50 kDa is the MsrA-GST fusion protein band.

Of the twenty colonies, eight showed the same fusion protein band intensity pre and post induction, suggesting that there was no change in the pre and post-induction expression such as shown by colony 1 in Figure 21.1. At 42°C, protein overexpression is temperature inducible and the growth condition of the cells at 37.5°C may be a small enough temperature difference so that cells are overproducing protein before IPTG was added. The induction tests showed experimentally that some E.*coli* colonies overproduced the MsrA-GST fusion protein before addition of the chemical inducer due

to the temperature induction factor.

To resolve this problem, the cells were grown at 30°C. Of the induction test colonies, colony five, showed optimal overproduction after the addition of IPTG (post-induction) and was grown up into a larger scale culture. 80% glycerol stocks were produced of the productive colonies and stored at -80°C.

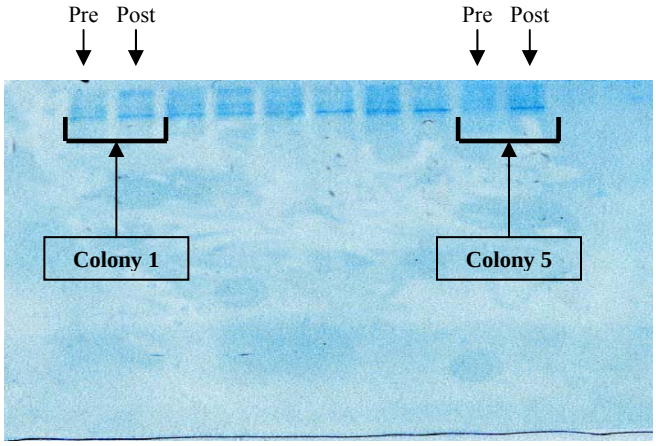

Figure 21.1. 15% SDS-PAGE analysis of MsrA-GST fusion protein expression in E. *coli* pre and post-induction.

Analysis of Purification and Protein Concentration

Isolated aliquots from each stage of protein purification were analyzed by 15% sodium dodecyl sulfate polyacrylamide gel electrophoresis (SDS-PAGE).

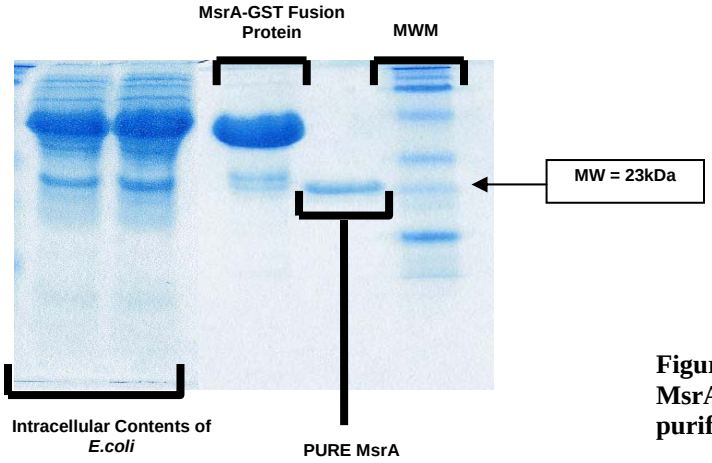

Figure 21.2. 15% SDS-PAGE analysis of MsrA-GST fusion protein expression, purification, and isolation of pure MsrA.

The concentration of MsrA was determined by UV-vis spectroscopy at A_{280} using the extinction coefficient $\varepsilon_{280} = 34{,}600\ M^{-1}cm^{-1}$.

The protein concentration was calculated using Beer's Law, $A = \varepsilon * \ell * c$ where:

A= Absorbance, $A_{280} - A_{350}$ (Absorbance units)
ε = Extinction coefficient ($M^{-1}cm^{-1}$)
ℓ = Path length (1 cm)
c = Concentration (M)

The absorbance (A) is determined by calculating the peak absorbance at 280 nm and subtracting the baseline absorbance value at 350 nm. Figure 21.3 shows a UV-vis spectrum of pure MsrA in PBS with a peak in the curve at 280 nm. This UV-vis scan shows that concentration of MsrA in this sample is 15.37µM.

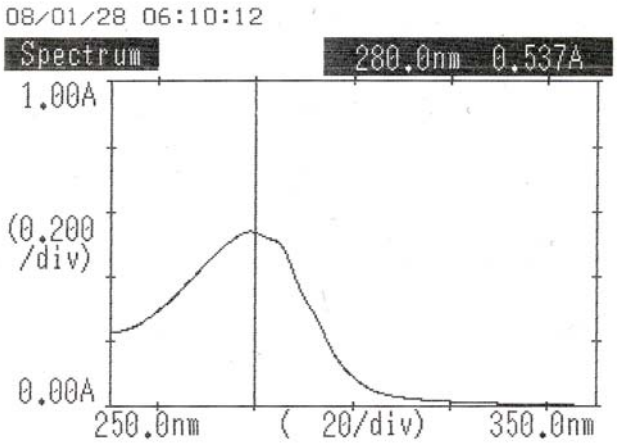

Figure 21.3. UV-vis spectrum of MsrA (15.37µM) in PBS scanned from 250 nm to 350 nm.

Preservation of MsrA Activity

Because MsrA is a catalytic antioxidant, the protein is very reactive in the oxygen environment under which it is studied. Oxidation of MsrA causes aggregation and renders the protein active site dysfunctional and unable to reduce the oxidized methionines of its substrate. A protocol was developed to wash the column-bound recombinant protein during the purification method with a solution of 5mM dithiothreitol (DTT) in PBS. The protein was then stored long-term in 5mM DTT in PBS. DTT is a reducing agent used for the reduction of disulfide bonds and restoration of the activity of sulfhydryl groups lost to oxidation. *In vitro,* DTT reduces the oxidized sulfhydryl by

thiol-exchange. Because DTT is needed to complete the catalytic cycle in MsrA kinetics studies, it must be removed from solution prior to fluorescence experimentation.